TRANSNAV the International Journal on Marine Navigation and Safety of Sea Transportation
http://www.transnav.eu
Volume 10
Number 2
June 2016

DOI: 10.12716/1001.10.02.06

Accuracy of Sea Ice Data from Remote Sensing Methods, its Impact on Safe Speed Determination and Planning of Voyage in Ice-Covered Areas

T. Pastusiak
Gdynia Maritime University, Gdynia, Poland

ABSTRACT: The data related to ice floe concentration and ice thickness were analysed. Sources of data have been verified by visual observation and by comparison in between information from different remote sensing sources. The results of this work exceeded initial expectations.
The discrepancies of the information provided by various data sources result from the error of the measurement method, which can be as high as 15% of the concentration of ice floes. It should also be borne in mind that the more generalized information about the state of the ice cover, the lower probability of detection of ice floe patches of a high concentration and spatial extent. Each vessel that is planning voyage in ice should take into consideration inaccurate estimation of concentration and thickness of ice floes received by means of satellite remote sensing methods. The method of determining permissible speed of various ice class vessel in ice on basis of safe speed graph for the icebreaker was developed. A well-defined equation approximates relationship between speed of the icebreaker and the vessels of specified ice classes.
Average distance of 24.1 Nm from sea ice extent line was related to all analysed lines representing 30-40% ice floe concentration (IUP product excluded) and 30.6 Nm for analysed lines representing 70-81-91% ice floe concentration. The maximal average distance of the furthest analysed line (IUP product excluded) was equal 37.2 Nm. The average standard deviation of that results was equal 8.3 Nm only. Average distances of analysed lines from sea ice extent line to maximal ice data values were found as follow: 8.4 Nm (23%) for NSIDC-CCAR ice age, 12.3 Nm (33%) for minimal distance of 30-40% ice concentration, 15.4 Nm (41%) for OSISAF ice type "ambiguous" zone from Open Water side, 25 Nm (67%) for minimal distance of 70-81-91% ice concentration, 26.6 Nm (72%) for OSISAF ice type "ambiguous" zone from 1st year ice age side, 35.9 Nm (97%) for maximal distance of 30-40% ice concentration and 36.3 Nm (98%) for maximal distance of 70-81-91% ice concentration data. In the parentheses placed relative distances from first ice data including IUP 40% concentration isolines. Sea ice extent of most of available data sources delineated the edge of "area to be avoided" for vessels of ice class lower than L1.
Estimated average speed of L3 ice class vessel was from 3.3 knots till 5.2 knots at average speed 5.0 knots. For L1 ice class vessel estimated average speed was from 6.5 knots till 12.1 knots at average speed 9.7 knots. Relative standard deviation of averaged speed for both ice class vessels was equal 18%. The highest relative deviations were found up to 50% below the average speed value. The highest relative deviations upward were equal 22%. Above speeds for L3 and L1 ice class vessels corresponded well with average technical speed of "Norilsk SA-15" ULA class vessel equal 12,6 knots.
The results of the work were not intended to be used for decision making on spot - "on-scene" - during direct guiding vessel in ice. They should be useful for initial voyage planning to allow decision-makers to identify the best freely available data sources for considered voyage and vessel of defined ice class; to understand advantages and limitations of available in the internet data sources; to estimate vessel's maximal safe speed in encountered ice conditions, to estimate spatial distribution and correlations in between various levels of sea ice concentration and thickness. All above data allow estimate voyage time that is, in addition to fuel consumption, basic criterion of maritime transport economics.

1 INTRODUCTION

Planning a voyage of a ship in ice-covered areas in the Arctic differs from the preparation of a standard one. The main threats to shipping are complex, variable in time and space ice conditions. They may, in extreme cases, completely disable the voyage in the whole route or part of it and potentially may pose a threat to its safety all the time.

A significant number of new sources of information characterizing the conditions for the Arctic ice appeared in recent years. They are obtained by means of satellite remote sensing methods. Some of them are compiled automatically, other are prepared with the support of highly qualified specialists. Properties and formats of these sources are very diverse. These sources are planned first and then analysed in detail in terms of their compliance with terrestrial observations. For this purpose, the results of visual observations of ice cover recorded in table of components of voyage plan, collected during the voyage of the vessel "Horyzont II" from Longyearbyen (78° 13' N, 015° 38' E) to Kinnvika (Murchisonfjorden, 80° 02' N, 18° 30' E) on the North of Svalbard on 10th of August 2009, and from Kinnvika to Longyearbyen on 15-16th of August 2009 were used. Routeing was determined on the basis of previously executed voyage. The map contents of the current ice conditions were not taken into account. The next step was to compare the consistency of data between the selected sources.

The results of the study should answer a few questions:

1 What data sources of ice concentration and ice thickness are freely available in nearly real-time for the region of interest?
2 What is the precision of the information and spatial distribution provided by each sea ice data source?
3 Is the scale of ice concentration and ice thickness presented by particular data source enough detailed for prediction of safe speed of a vessel in ice?
4 What is the usefulness of particular sources for planning of route and schedule consecutively appointed after each trip?
5 Is the usefulness of particular sea ice data sources the same for each ice class of vessels?
6 Could vessel determine more favourable route if the content of sea ice data sources was taken into account?
7 Could vessel avoid movement through the field of higher concentration of ice floes at the initial stage of planning the route?
8 Is possible to define equation that approximates relationship between speed of the icebreaker and the vessels of specified ice classes?
9 Is possible to extract general relationships in between various sea ice concentration and thickness isolines that will be useful for initial voyage planning?

2 PRELIMINARY ASSUMPTIONS AND RESEARCH METHOD

Concentration and thickness (age or type) of ice were adopted as basic parameters of ice to choose optimal route of the vessel (Arikaynen & Tsubakov 1987, Arikaynen 1990). Canadian administrative method of assessing the feasibility of the vessel passage in ice is based on ice class of the vessel, the concentration and age of ice utilizing ice numeral method (Timco at all 2005, Canadian Hydraulics Centre 2003). Canadian Ice Services provide ice charts on CIS web site for concentration of ice pack and stage of ice development. Russian Federation also adopted administrative method of assessing the feasibility of the vessel passage through particular NSR seas (RMSR 2015). In this case the criteria are ice class of vessel, period of year and ice conditions (extreme, hard, medium and easy). AARI publishes ice concentration maps in the summer time on ESIMO web site. Maps of ice thickness (age) are published during the winter time.

Concentration and thickness of ice were adopted as a criterion of ice maps evaluation. Vessels are built according to the planned conditions of navigation in ice. AARI criterion of "ice-free" navigation capability was also taken into consideration when assessing the ability of the vessel with specified reinforcements of the hull structure for navigation in ice (Table 1).

Table 1. Capability of 'ice-free' navigation in Arctic waters for various ice class vessels (following Arikaynen, 1987)

Ice Class	Criteria of "ice-free" navigation capability
Icebreakers or ULA with icebreaker's assistance	Ice pack concentration CT > 70-80%
ULA (without Norilsk class ships)	Ice pack concentration CT ≤ 70-80%
UL, L1	Ice pack concentration CT ≤ 40-60%
L2, L3, L4	Ice pack concentration CT ≤ 10-30%

2.1 *Precision of determined sea ice conditions from data sources derived from remote sensing methods*

At first, compliance of the information presented on maps derived from remote sensing methods with visual and radar observations made on the vessel was verified. Then, the compliance of ice floe concentration edges from various sources received by remote sensing methods were verified. For this purpose were used available online files in JPG and GeoTIFF raster formats and in GRIB and NetCDF grid formats as well as in Shapefile / SIGRID-3 vector format. The raster format maps were calibrated. Routes of the vessel and ice floe field boundaries obtained from visual and radar observations have been saved in Shapefile format. This allowed the data contained in all files to be visualized on a single screen in a georeferenced system.

Displaying all examined maps from remote sensing and observed ice floe field boundaries found by the vessel on a single screen was designed to facilitate the comparison of results from different sources of information and to increase the accuracy of

the position and parameters of the ice cover. On this basis, it was intended to determine which sources of information more accurately visualize the actual limits of ice floe concentration fields as to the value of concentration, position and spatial distribution. In this way it was intended to determine which files (maps) are best suited on board of conventional vessel, non-conventional vessel, a yacht or a boat or ashore in the owner's office or planner's office in voyage planning in ice-covered areas.

The work is a scientific analysis. That is why sources of information were not divided into the official (derived from authorized nautical providers) and unofficial (for scientific climate research). It was expected that the qualitative diversity of information sources will result from the correctness and accuracy of georeferenced files, resolution and precision of concentration and thickness of scale used. This diversity should also comprise the width of filtered band around land (omitted when making the map) and the value added to automatic results by the scientists (who develop maps). Finally, this diversity should verify information from remote sensing data by means of visual and radar observations made by the author of the work that carried out during the voyage of the vessel in the North of Svalbard.

Conditions observed on board vessel were recorded by taking video of the radar screen and by taking pictures of visual view of sea surface ahead of the vessel. The most difficult ice conditions were identified by means of recorded waypoints position, speed of the vessel and concentration of ice floe. Positions and parameters of the detected edges of ice floe patches of higher concentration and theirs thickness (pictures 3a, 3b) were also reconstructed. The speed of the vessel in the ice was the smaller, the greater the concentration of ice floe was. Full speed of 11 knots reflected lack of ice in the vicinity (0.5 - 1 Mm). Reduced speed of 6 knots indicated navigation in the area of ice floe concentration below 35%. Reduced speed below 3.5 knots was connected with navigation in close proximity of ice. The speed was below 2.5 knots when passing through the field of ice floe of concentration above 50%.

2.2 *Difference in travel time estimation resulting from inaccuracies of determined speed of vessel in ice*

Second matter raised in this work was influence of discrepancy in between ice cover parameters presented by data sources from remote sensing methods and real ice conditions on estimation of time required for the voyage. Ice data sources from remote sensing may serve for initial voyage planning, including speed and time required to complete whole voyage.

The IMO included vessel speed related to individual parameters of ice conditions in Ice Passport. These data are approximate and support the decisions of the vessel's captain. If the vessel does not have Ice Certificate (Ice Passport), it is necessary to determine the maximum safe speed as a function of ice conditions. This issue can be solved in an approximate way. Two parameters were used to determine the speed of the vessel. These are the concentration and thickness of ice – the most frequently available data. Availability of these parameters allows to use Arikaynen nomogram (1990). This nomogram is used to estimate the speed of the vessel (the icebreaker) in the Russian Arctic. Mathematical equation was developed for more precise and more convenient computing of speed of the vessel in the ice instead of using Arikaynen nomogram. First, the speed, concentration and thickness of the ice on a nomogram stored in a table in a text file. So summarized data were analyzed searching three-dimensional data nearest approximation method of least squares using "TableCurve 3D" software. At first, searched for mathematical formula that allows direct calculation in MS Excel spreadsheet. Secondly, searched for a three-dimensional mapping, which will be the most coincident with the speed distribution for zero values for concentration of ice and the most coincident with the speed distribution for zero values of ice thickness. It was chosen equation for the top position (rank) that met the requirements listed above (Equation 1).

$$V_i = a + b \cdot x + c \cdot y + d \cdot x^2 + e \cdot y^2 + f \cdot x \cdot y \qquad (1)$$

where V_i = speed of the icebreaker in knots; x = concentration of ice floe in percent; y = thickness of ice in meters; and coefficients a = 22.638294; b = 0.061043651; c = − 0.025492605; d = − 0.00094047619; e = 0.00011634199; f = − 0.0010144048.

Parameters of transformation are as follow: r^2 = 0.99056544, *Degree of Freedom Adjusted* r^2 = 0.98936102, *Fit Standard Error* = 0.5920998, *F-statistic* = 1007.9351. The highest relative values of residuals are equal 67.57215, 12.740919 and 19.842322 % (for concentration = 100% and thickness 180 cm, 160 and 140 cm respectively). Due to low absolute values of speed at these points, the absolute value of residuals is also low like at other points. They are far away from concentration and thickness allowed for vessels of low ice class L4 till L1 (RMRS 2015). Twelve data points are in the range 9.097 – 4.211 %. Next ones are in the range between 3.890 and 0.035 %. For comparison purposes, the transformation parameters for equation of the highest position named „Chebyshev X, Y Bivariante Polynominal Order 5" are as follow: r^2 = 0.99827402, *Degree of Freedom Adjusted* r^2 = 0.99714135, *Fit Standard Error* = 0.30543242, *F-statistic* = 954.33037. The highest values of residuals are equal 13.36013 % and 11.331476 %. Next ones do not exceed value of 3.547791 %. Based on a comparison of transformation parameters for both models assumed that Equation 1 accurately reflects the Arikaynen (1990) nomogram.

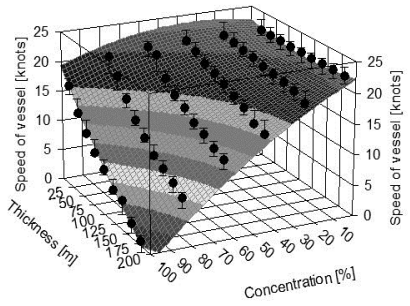

Figure 1. Surface-fit graph of ice floe concentration and thickness and technical speed of the vessel in. Developed by author based on Arikaynen nomogram (1990).

Table 2. Relationship in between ice class of vessels, ice floe concentration, ice thickness and speed correction factor F. Developed by author based on RMRS 2015 and Equation 1.

Ice class	Concentration	Thickness	Factor F
	[%]	[cm]	---
Ice1 (L4)	60	40	0.25
Ice1 (L4)	100	35	0.20
Ice2 (L3)	60	55	0.27
Ice2 (L3)	100	50	0.26
Ice3 (L2)	60	70	0.29
Ice3 (L2)	100	65	0.26
Arc4 (L1)	70	80	0.52
Arc5 (UL)	70	100	0.58
Arc6	90	130	0.68
Arc7 (ULA)	90	170	2.00

To determine the speed of vessels of lower ice classes on the basis of Arikaynen nomogram should be used speed correcting factor F. Value of the factor F depends on vessel's ice class, concentration of ice floe and thickness of ice. It was determined value of speed correcting factor F (Table 2) following rules included in RMRS (2015). Value of factor F is of clearly different range for vessels of low ice class (L4 – L2) and vessels of medium ice class (L1 – ULA). The technical speed of vessel of lower ice class can therefore be estimated from Equation 2. It was found relatively high value of factor F for ULA class vessels due to unknown reason. Therefore assumed ULA class data presented in Table 1 to be unreliable.

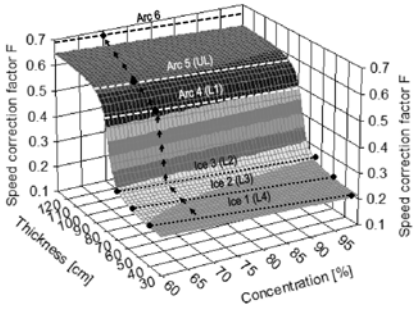

Figure 2. Speed correcting factor for various ice class vessels

$$V_t = F \cdot V_i \tag{2}$$

where V_t = technical speed of vessel; V_i = speed of the icebreaker according to Equation 1; F = speed correcting factor.

3 CHARACTERISTICS OF THE DATA SOURCES USED IN THE STUDY

3.1 *The NIS maps of ice concentration in raster JPG format with geographic coordinates*

The producer of these maps is the Norwegian Ice Service (met.no). The maps are developed on the basis of SAR images of European and Canadian RADARSAT and ENVISAT satellites at a resolution of 75-150 meters. Spatial resolution of these charts is 1.000 m (NIS, http://polarview.met.no/documentation.html). In this way they allow determination of ice conditions in the fjords and straits which have a width of a few kilometres only. The files adopt a standard name c_map3.jpg. Examined files were downloaded from the website http://polarview.-met.no/. The scale of ice concentration is discrete and includes the following information: Open Water (CT = 0-10%), Very Open Drift ice (CT = 10-40%), Open Drift ice (CT = 40-70%), close Drift ice (CT = 70-90%), Very Close Drift ice (CT = 90-100%), Fast ice.

3.2 *The NIC vector maps of the ice concentration, ice age and floe size in PDF or Shapefile format*

These maps are actually discontinued. The producer of these maps was the US National / Naval Ice Center. Examined files were downloaded from the website http://www.natice.noaa.gov/products/ weekly_products.html and tab "Barents Sea NW". These maps are available in vector PDF format (files named barnwYYMMDDcolor.PDF with plotted geographic coordinates) or in vector Shapefile format (file named barnwYYMMDD.zip which contains SHP, DBF, SHX, and PRJ files). The files contained particular data on weekly or bi-weekly basis. They represent the ice conditions for the week in which they were published. Data for the analyses went back 96 hours from when they were completed. They were dated with the week they were published. Additional information included in the scale determined: Fast ice, Ice shelf, Undefined. They were based on an analysis and integration of all available data on ice conditions, including weather and oceanographic information, visual observations from shore, ship and aircraft, airborne radar, satellite imagery (RADARSAT, ENVISAT, MODIS, and GMM) and climatological information. These products were mainly used for climate analysis, climate change studies and as input to the Global Digital Sea Ice Data Bank (GDSIDB) but they can also provide ice information to marine community to enhance the safety and the efficiency of marine operations in ice covered waters.

3.3 *The AARI maps of concentrations, age and of ice forms in vector Shapefile format*

The producer of these maps is the Ice Center AARI. They are compiled on the basis of satellite information (in the visible, infrared and radar bands) and reports from the Arctic and coastal stations same like ships. The data are collected during the period of 2-5 days and after averaging are issued every Thursday which is the reference date. An example name of file is aari_bar_YYYYMMDD_pl_a.ZIP (which contains

SHP, DBF, SHX, PRJ files) elaborated for the Barents Sea. Maps of concentration, age and forms of ice for the Arctic Ocean in vector SIGRID-3 format with a sample name aari_arc_YYYYMM-DD_pl_a.ZIP (which contains SHP, DBF, SHX, PRJ files) are taken into account as equivalent maps. Examined files downloaded from the website http://www.aari.ru/projects/ecimo/index.php?im=10-0. Scale of the map is 1: 5,000,000 (adopted on the basis of its raster equivalent). It should be noted that the raster equivalent map for aari_arc_YYYY-MMDD_pl_a.ZIP file is drawn up on a scale of 1: 10,000,000.

3.4 *The IUP maps of the concentration of ice in raster GeoTIFF format*

The producer of these maps is the Institute of Environmental Physics, University of Bremen. The maps are developed on the basis of AMSR-E images (currently AMSR2) using the ASI algorithm. The resolution of these maps is equal to 3.125 meters. An example name of file is asi-n3125-YYYYMMDD.tif. The examined files were downloaded from the website http://iup.physik.unibrmen.de:8084/amsredata/-asi_daygrid_swath/l1a/n3125/. The scale of visualized ice concentration is available on website http://iup.physik.uni-brmen.de:8084/amsredata/asi_-daygrid_swath/l1a/n3125/2009/aug/Svalbard/asi-n3-125-0090810_nic.png and on website http://iup.-physik.uni-brmen.de:8084/amsredata/asi_daygrid_-swath/l1a/n3125/README.TXT. Colours of the scale reflect increments of concentration for every 10% for a value between 0 and 80% and for every 5% of values between 80 and 100%. Global Mapper software displays digital value increments of concentration of 0.5%. However, the unit of the displayed parameter is not displayed.

3.5 *The NIC "daily products" maps of the MIZ ice concentration scale in vector Shapefile format*

The producer of these maps is the National Ice Center (US). They are compiled from a variety of sources with a resolution better than 50 meters per pixel. Sources of information include (but are not limited to) ENVISAT, DMSP OLS, AVHRR i RADARSAT (http://www.natice.noaa.gov/ products/-daily_products.html). The NIC analysts carry out the necessary interpretation of images that improves the value of these sources for the correct identification of the extent of the ice edges. An example name of files is nic_mizYYYYDDDnc_pl_a.zip (which include SHP, DBF, SHX, PRJ files) drawn up for the entire Arctic Ocean. Examined files were downloaded from the website http://www.natice.noaa.-gov/products/daily_- products.html and tab "MIZ Shape". The scale of ice concentration is available on website http://www.natice.noaa.gov/produts/pro-ducts_on_demand.html. Field CT81 means concentration above 80%, CT18 (Mariginal Ice Zone) means concentration between 18% and 80%, "Open water" means concentration of ice floe from zero to 17%.

MIZ maps issued by NIC (products on demand) on the concentration of ice for the Arctic Ocean in vector Shapefile format show identical edge lines. An example name of files is arctic_daily_MMDDYYYY. Examined files were downloaded from the website http://www.natice.-noaa.gov/products/products_on_demand.html. Information concerning these files is consistent with the data described in the related files nic_mizYYYYDDD-nc_pl_a.zip. The research made use of nic_miz-YYYYDDDnc_pl_a.zip files.

3.6 *The NCEP maps of ice concentration in gridded GRIB format in a resolution of 5 minutes of arc*

The producers of these maps are the NWS, NOAA, NCEP, NOMADS. Spatial resolution of these maps is 5′ of latitude by 5′ of longitude (geographical greed). Examined files were downloaded from the website ftp://polar.ncep.noaa.gov/cdas/archive/. An example name of files is ice5min.YYYYMM.grb. This file contains particular data for each day of the month. The scale of ice floe concentration is continuous in the range between 0 and 100% with increments of one percent. Additional scale includes the following information: Land, Weather, Bad data, Coast, No data (Grumbine R, 1996, ftp://polar.ncep.-noaa.gov/pub-/pub/mmab/papers/ ssmi120.ps.gz).

3.7 *The IFREMER maps of ice concentration in gridded NetCDF format without geographical coordinates plotted*

The producer of these maps is the CERSAT that is part of IFREMER. They are compiled on the basis of satellite SSMI and QUIKSSCAT images. Spatial resolution of these charts is 12,500 meters (Erzaty and others, 2007). An example name of file is YYYYMMDD.nc. Examined files were downloaded from the website ftp://ftp.ifremer.fr/ifremer/cersat-/products/gridded/psi-concentration/data/arctic/daily/netcdf/2009/. In order to eliminate the pixels associated with the land, grid masks have been enlarged up to two pixels (25 miles) away from the land. In connection with the use of weather filter, an area considered to be free of ice is determined by the 15% ice concentration limit. The scale of ice floe concentration is continuous in the range between 0 and 100%.

3.8 *The NIC maps of the sea ice extent and sea ice edge boundary in vector Shapefile format*

The producer of these MASIE maps is the NIC. These charts use a wide variety of data sources such as MODIS, AVHRR-VIS, GOES, SEVIRI, MTSAT, AMSR-E, SSM/I, AMSU, SAR imagery from RADARSAT-2, ERS-2, ALOS, PALSAR, ASAR. The ice charts and ice edge products from ice charting agencies in the US, Canada, Norway, Denmark, Russia, Germany, Sweden and Japan also serve as data sources in the absence of direct satellite data. These charts are constructed by analysts trained in remote sensing imagery interpretation and sea ice climatology. Spatial resolution of these charts is 4 km. An example name of file is masie_ice_r00-

_v01_YYYYDDDD_4km.ZIP (containing SHP, SHX, DBF and PRJ files). Examined files were downloaded from the website http://nsidc.org/data/-docs/noaa/g02186_masie/index.html. The analysts integrate all data sources for the best estimate of spatial coverage of ice cover. A cell is considered ice covered if more than 40 percent of the 4 km cell is covered with ice. This is regardless of the ice thickness or ice type. It is worth mentioning that the daily ice edge product is used to warn navigators and others in the Arctic where ice exists or is likely to form at any concentration. The primary users of the ice charts and ice edge products are marine transportation interests. The input product for MASIE is IMS product that is designed primarily for modellers. It is produced relatively consistently in comparison with chart and edge products. It also benefits from the same careful manual analysis that is used for chart and edge products.

3.9 *The OSISAF maps of ice concentration in gridded NetCDF format with geographical coordinates*

The producer of these maps is the EUMETSAT Ocean And Sea Ice Satellite Application Facility, High Latitude Centre (osisaf.met.no). Is being implemented by a consortium CDOP established by Meteo-France, as managing authority. Implementing bodies are: Met.no (Norway), DMI (Denmark), IFREMER (France), KNMI (Holland) and SMHI (Sweden). These maps are developed with EUMETSAT satellite images on the basis of SAF program. The sea ice concentration product uses SSMIS data. Spatial resolution of these maps is 10,000 meters. An example name of file is ice_conc_- nh_polstere-100_multi_YYYYMMDDHH00.nc. Examined files were downloaded from the website ftp://osisaf.met.no/archive/ice/conc/2009/08/. The limit between water and open drift ice is defined to be 35% ice concentration. Scale of ice floe concentration continuous in range of 0 to 100%. Additional information of scale include: Over land, Unclassified or No data. They are described on web site http://osisaf.met.no/docs/osisaf_ss2_pum_ice-conc-edge-type.pdf (Eastwood 2014). It must be highlighted, that the only navigation ice charts based on subjective interpretation of high resolution SAR, MODIS and AVHRR data are used in the evaluation of the OSI SAF products.

The same information on ice floe concentration contain gridded GRIB type files named ice_conc_nh_201105211200.grb.gz of same producer. For this reason, they were not analysed in the work.

3.10 *The OSISAF maps of ice concentration in gridded NetCDF format in simlified scale with geographical*

The producer of these maps is the EUMETSAT Ocean And Sea Ice Satellite Application Facility, High Latitude Centre (osisaf.met.no). Is being implemented by a consortium CDOP established by Meteo-France, as managing authority. Implementing bodies are: Met.no (Norway), DMI (Denmark), IFREMER (France), KNMI (Holland) and SMHI (Sweden). Multi sensor methods with a Bayesian approach is used to combine SSMIS and ASCAT data for ice concentration simplified (edge) classification. Spatial resolution of these maps is 10.000 meters. An example name of file is ice_edge_nh_- polstere-100_multi_YYYYMMDDHH00.nc. Examined files were downloaded from the website ftp://osisaf.met.no/archive/ice/edge/2009/08/. The limit between water and open drift ice is defined to be 35% ice concentration. The limit between open drift ice and close drift/very close drift ice is defined around 70 % ice concentration. Thus defined, simplified scale MIZ includes the notions of: Ice free (CT = 0-35%), Open ice (CT = 35 -70%), Closed ice (CT = 70-100%). Additional information of scale include: Over land, Unclassified or No data (OSISAF 2009). They are described on web site http://osisaf.met.no/docs/osisaf_ss2_pum_ice-conc-edge-type.pdf (Eastwood 2014). It must be highlighted, that the only navigation ice charts based on subjective interpretation of high resolution SAR, MODIS and AVHRR data are used in the evaluation of the OSI SAF products.

The same information on ice floe concentration contain gridded GRIB type files named ice_edge_nh_201105211200.grb.gz of same produc-er. For this reason, they were not analysed in the work.

3.11 *The OSISAF maps of ice type in gridded NetCDF format with geographical coordinates*

The producer of these maps is the EUMETSAT Ocean And Sea Ice Satellite Application Facility, High Latitude Centre (osisaf.met.no). Is being implemented by a consortium CDOP established by Meteo-France, as managing authority. Implementing bodies are: Met.no (Norway), DMI (Denmark), IFREMER (France), KNMI (Holland) and SMHI (Sweden). They are developed from EUMETSAT satellite images. An example name of file is ice_type_nh_polstere-100_multi_YYYYMMDDH-H00.nc. Examined files were downloaded from the website ftp://osisaf.met.no/archive/ice/type/2009/08. They are described on web site http://osisaf.met.no-/docs/osisaf_ss2_pum_ice-conc-edge-type.pdf (Eastwood 1014)).

Sea ice data are daily means centered for time moment of 12:00 UTC (noon). Spatial resolution of these charts is 10.000 meters. The limit of data is the limit in between water and open drift ice and defined to be 35% ice concentration (OSISAF 2009). Multi sensor methods with a Bayesian approach is used to combine SSMIS and ASCAT data for ice type classification. It must be highlighted, that the only navigation ice charts based on subjective interpretation of high resolution SAR, MODIS and AVHRR data by skilled analysts are used in the evaluation of all OSI SAF products (concentration, edge and type). The map identify following classes: first-year, multi-year sea ice and "uncertain". During summer period from June to September, when the first-year ice decreases or becomes multi-year ice, the distinction between ice types is difficult due to ice melting (wet ice and water on the ice). In case no information on ice type in the data, the ice type is classified as "uncertain".

False ice filtering is implemented by setting all grid points with temperature on 2 meters level >8.0°C

to open water. To avoid the improper removal of extreme ice extents, the NSIDC climatological maximum of sea ice edge is extended towards open water by 50 km. This sea ice edge (determined by the 15 % ice concentration contour) from the day before, is expanded towards open water by 100 km and added.

The same information on ice floe concentration contain gridded GRIB type files named ice_type_nh_201105211200.grb.gz of same produc-er. For this reason, they were not analysed in the work.

3.12 *The NSIDC-CCAR maps of sea ice age in raster GIF format*

Data were originally provided by Mark Tschudi, CCAR, University of Colorado, UCB 431, Boulder, Colorado, USA, provided via Stefan Kern, Integrated Climate Data Center (ICDC, http://icdc.zmaw.-de), University of Hamburg, Hamburg, Germany. They are described on web page http://icdc.-zmaw.de/seaiceage_arctic.html?&L=1 and http://n-sidc.org/data/docs/daac/nsidc0611-sea-ice-age/#de-rivtechnique (attempt 15.03.2015). Examined file was named age2009_33.GIF. Spatial resolution of the grid was 12.5 km. Sea ice age data are weekly means.

It was assumed the age of ice from 1 till 5 years represent mean thickness of ice 1.49 m, 2.02 m, 2.28 m, 2.47 m and 2.68 m (Maslanik at all. 2007). The changes in age and thickness in the period 1997-2007 reflect loss of ice in the Chukchi and Beaufort seas earlier in this period, combined with losses in the East Siberian Sea during the last 4 years. Over that 10 years, thickness associated with ice age has increased in the Laptev Sea, the Fram and the Nansen basins, which were previously regions of ice loss (from the late 1980s till mid 1990s).

The sea ice age data were estimated by using data from satellite passive microwave instruments (SMMR, SSMI, SSMIS), drifting buoys (IAPB) and a weather model (NCEP/NCAR/CDAS). AVHRR data were used in 2014 also. The formation, movement and disappearance of sea ice was observed using these data. Same in turn was used to estimate ice age (Maslanik et al. 2007).

More detailed, sea ice concentration and sea ice drift were used to investigate sea ice drift. Sea ice extent was calculated for every week. Only grid cells with at least 40% of sea ice concentration were used in the computation to minimize inclusion of artefacts. Largest uncertainties to be expected during melt period and in the Marginal Ice Zone when and where sea ice concentration and drift have the largest uncertainties.

Each of above mentioned grid cells were treated as particle which moves according to the weekly sea ice drift. The position of that cell is tracked for every week and the number of weeks was counted. Every year in between week 37 and 38 (September), upon commence of freezing conditions the age of still existing grid cells is rounded up to the successive full year. To be noted, first-year sea ice means in the current winter, second-year sea ice has survived one melting season, third-year sea ice has survived two melting seasons, and so on. No minimum thickness nor range of each age thickness nor decay of ice were taken into consideration by the author during current analysis of the work.

4 VISUAL OBSERVATIONS

In August 2009, the ship "Horizon II" performed a return voyage from Longyearbyen to Kinnvika within the ongoing project IPY-58 KINNVIKA and special project 111/IPY/2007/01. The hull of the vessel meets the criteria for ice class L1. Due to the lower main engine power the ice class of the vessel is reduced to L2. During this voyage visual and radar observations of hydro-meteorological and ice conditions were made, as well as the records of ship motion parameters from safety of navigation point of view. These conditions documented through photographs and videos of the vessel's surroundings and the radar screen. The identified parameters are presented separately in the tables for the voyage from Longyearbyen to Kinnvika (Table 3) and for the voyage from Kinnvika to Longyearbyen (Table 4). High values of concentration are related to the places where the vessel passed through or passed in vicinity of ice edge. Three locations of higher concentration of ice floe were found on the way to Kinnvika. Only one place was found during way back. The edges of a higher concentration of ice had sequentially assigned name, date and time: Edge-1 - 2009.08.10 12:00 UTC, Edge-2 - 2009.08.10 13:25 UTC, Edge-3 - 2009.08.10 15:45 UTC and Edge-4 2009.08.14 14:30 UTC. For each of these places sketch of the ice floe edge was made. They were then stored in a Shapefile file. The spatial distribution of the observed ice edge and implemented vessel routes are shown in Figure 3.

The sea ice thickness also was taken into consideration. Ice floe freeboard in vicinity of the vessel evaluated equal normally from 10 cm to 20 cm with inclusions of hummocked floe with average freeboard of 50 cm. It was same at the limits of ice floe fields Edge-1 to Edge-4. Only in exceptional cases found inclusions of hummocks reached up to 80 cm. There was found higher ice floe freeboard at the centre of analysed ice floe fields and in the ice Floe fields far away North from the route of the vessel. Following above observations the sea ice floe thickness (high) was estimated equal from 36 to 72 cm with inclusions of hummocked ice floe 180 cm high, in exceptional cases 288 cm.

Table 3. Voyage plan table from Longyearbyen to Kinnvika

Way-Point	Long. E [°]	Lat. N [°]	Speed [knots]	Concentration [%]	Floe size [meters]
22	80.1405	14.1171	11.1	0	0
23	80.1475	14.3073	11.1	70 (Edge-1)	110
24	80.1285	14.4828	11.1	40 (Edge-1)	70
25	80.1285	14.5555	11.1	30 (Edge-1)	70
26	80.1295	14.8633	11.0	20 (Edge-1)	110
27	80.1208	15.0516	11.1	1	70
28	80.1298	16.5333	11.2	0	0
29	80.0391	17.4273	8.4	1	70
30	80.0310	17.5203	5.1	70 (vessel out of Edge-2)	110
31	80.0308	17.5750	9.0	70 (vessel out of Edge-2)	110
32	80.0096	17.6745	10.9	5 (vessel out	20

				of Edge-2)	
33	80.8333	17.7133	11.1	40 (vessel out of Edge-2)	90
34	80.0053	17.7190	8.7	1	40
35	80.0053	17.7461	10.4	1	40
36	80.0048	17.8013	5.1	5	40
37	80.0103	17.8558	1.8	60 (Edge-3)	70
38	80.0130	17.8851	3.2	60 (Edge-3)	70
39	80.0096	17.8920	1.3	40 (Edge-3)	70
40	80.0103	18.0640	3.1	40 (Edge-3)	70
41	80.0156	18.0800	1.4	40 (Edge-3)	70
42	80.0135	18.1215	0.5	40 (Edge-3)	70
43	80.0148	18.1323	1.3	50 (Edge-3)	54
44	80.0168	18.1531	3.4	40 (Edge-3)	50
45	80.0233	18.1648	1.5	30 (Edge-3)	50

Table 4. Voyage plan table from Kinnvika to Longyearbyen

Way-Point	Long. E [°]	Lat. N [°]	Speed [knots]	Concentration [%]	Floe size [meters]
1	18.2007	80.0335	6.0	2	50
2	18.1229	80.0130	11.3	4	33
3	18.0283	80.0093	11.3	4	33
4	17.8818	80.0117	11.3	4	55
5	17.7750	80.0075	11.3	4	40
6	16.4837	80.1311	11.3	1	33
7	15.4168	80.1260	11.3	0	0
8	15.1554	80.0843	11.3	25 (Edge-4)	33
9	15.0587	80.0910	10.4	60 (Edge-4)	90
10	15.0139	80.0941	4.0	65 (Edge-4)	83
11	14.9870	80.0965	11.0	2	50
12	14.9215	80.1036	11.0	2	50
13	14.8945	80.1069	6.0	2	70
14	14.8624	80.1093	1.2	6	70
15	14.8329	80.1115	8.2	2	70
16	14.7701	80.1148	11.3	1	50
17	14.7392	80.1165	11.3	1	50
18	14.6918	80.1180	11.3	1	70
19	14.5586	80.1205	11.3	1	50
20	14.3460	80.1222	11.3	1	50
21	14.0571	80.1206	11.3	1	50
22	13.9682	80.1159	11.3	1	50

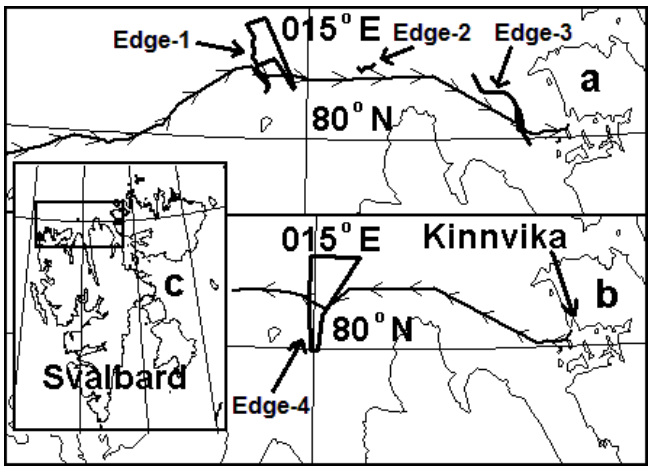

Figure 3. The vessel's routes North of Svalbard and observed ice floe edges: a – route towards Kinnvika, b – route towards Longyearbyen, c – area covered by the research. Symbols: —►— route towards Kinnvika, ◄— route towards Longyearbyen, ——— edge of ice pack. Ice floe edges marked respectively (Edge-1, Edge-2, Edge-3, Edge-4).

5 DISCUSSION OF RESULTS

5.1 *Verification of information from remote sensing using visual observations*

Only few data sources were in vicinity of vessel's route. Most of them were out of sight. However the characteristic shapes of the edge of all sources were analysed. Searched correlations (or lack of correlations) and distances in between patterns.

5.1.1 *NIS maps of the concentration of ice in raster JPG format with geographic coordinates plotted*

Map named c_map3.jpg was assessed. The exact time of the NIS map was not specified. Therefore the date indicated on the map equivalent sarmap2.jpg - 2009.08.10 08:47 UTC was adopted. The ice edge (CT = 40-70%) shown on the NIS map is observed from the vessel offset of ice edge (Edge-1) of 4.0 Nm in the direction 000°. The map did not demonstrate the existence of an ice floe wedges with a width of less than 1.0 Nm. The ice edge (CT = 40-70%) shown on the NIS map is observed from the vessel offset of ice edge (Edge-2) of 4.4 Nm in the direction 046°. The ice edge (CT = 40-70%) shown on the NIS map is observed from the vessel offset of ice edge (Edge-3) of 2.6 Nm in the direction 113°. The map did not demonstrate the existence of an ice floe wedges with a width of less than 0.3 Nm. It seems that NIS map is offset, in relation to all three observed from the vessel, of ice floes edges of higher concentrations in different directions. Average offset distance was 3.7Nm. The time difference between successive ice edges abeam of the vessel was 1.4 hours and 2.3 hours. They showed an increasing delay in relation to the publication of the NIS map by 3.2 hours, 4.6 hours and 6.9 hours.

Map named c_map3 dated 2009.08.14 14 06:30 UTC used for comparison with the edge of the ice floes observed from the vessel (Edge-4) was dated 2009.08.14 22:30 UTC. The ice edge (CT = 40-70%) and field of ice floe of concentration CT = 10-40% that is shown on the NIS map were offsets from the vessel observed ice edge of the concentration of 25-60% (Edge-4) of 2.4 Nm in the direction 042°. It seemed that the scale of the ice concentration of the NIS map depicted accurately the spatial distribution of ice observed from the ship. The undetected field of ice floe of higher concentration with a width of 1.5 Nm are presented in Figure 4. It was included inside the field with a concentration of CT = 10-40%. It was assumed that NIS map in an accurate way depicted the state of the ice cover at the time of reference for the source data.

5.1.2 *Vector NIC map of the ice concentration, ice age and floe size in PDF format*

These maps were published at intervals of 14 days. The closest map corresponding to the observation date was ice edge map dated 2009.08.17. For this reason, only Edge-4 referenced to the date 2009.08.14 22:30 UTC was analysed. The time difference was 49.5 hours (equal to 2.06 days). Map of 2009.08.03 (mean time of source data dating 2009.08.04 0:00 UTC) showed a general ice drift in the direction of 253 ° with an average distance of 20 Nm in seven days.

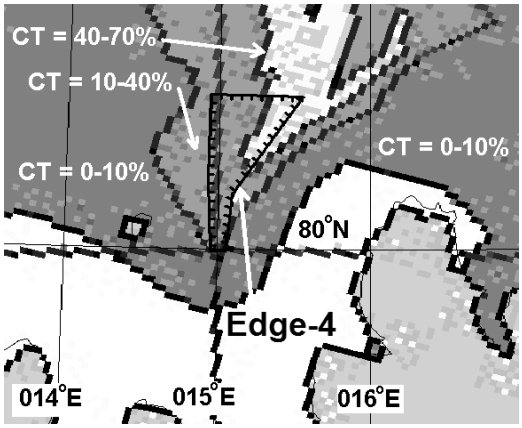

Figure 4. Location of ice cover according to NIS c-map3 map dated 2009.08.14 06:30 UTC and ice floe edge observed from ship

Map of 2009.08.17 (average time of data source dating 0:00 UTC) showed a general ice drift in the direction of 245 ° at an average speed of 35 Nautical miles in seven days. This means drift ice equal to 10 Nautical miles of the time difference between visual observations and the dating of the ice edge map source data. After moving, the ice edge position on the map of a concentration of 40-60% for estimated resultant drift ice noted the consistency of data in comparison with the observed Edge-4 (Figure 5).

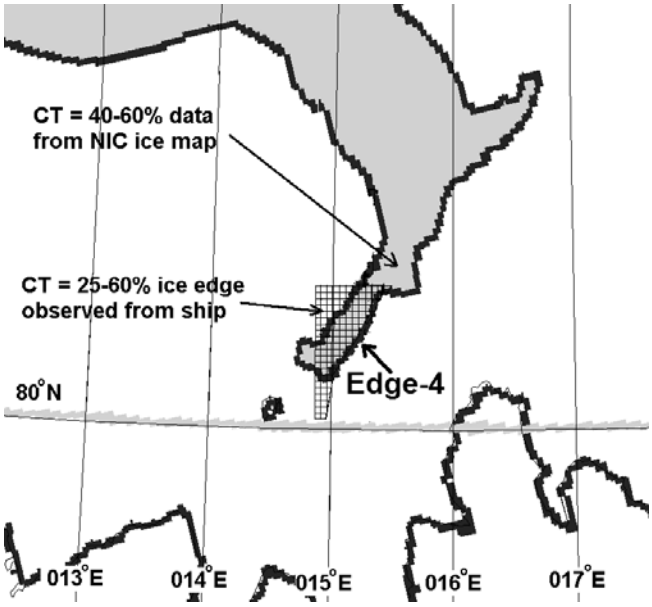

Figure 5. Locations of ice cover according to NIC barnw090817color map and ice floe edge observed from ship after approximate adjustments of time difference and drift of ice cover.

It was assumed that the NIC map accurately reflects the state of the ice cover for reference time of the data source. It was assumed that remote sensing method did not detect the ice pack field with a width of less than 1.5 Nm. When only the information about the ice drift from the map dated 2009.08.17 was considered, the position of the edge of the ice floe would be shifted 16 Nm in the direction of 130 ° with respect to the observed ice floe edge from the vessel.

5.1.3 *AARI maps of concentration, age and ice forms in vector Shapefile format*

The aari_bar_20090811_pl_a (SHP, SHX, DBF, PRJ) file was used for comparison with the observed from the vessel ice floe field edges dated respectively Edge-1 (2009.08.10 12:00 UTC), Edge-2 (2009.08.10 13:25 UTC) and Edge-3 (2009.08.10 15 45 UTC. It was assumed that the map represented ice conditions dated 2009.08.10 12:00 UTC because it reflected the average ice cover for the last three days. Another assumption was made that the time difference equal to 0-3.75 hours is negligible. Edge-1 field had no equivalent on the AARI map. The closest edge of the ice floe field of concentration CT = 13% on AARI map, that was coincident with shape of the Edge-1, was located at a distance of 6 Nm in the direction of 350°. The closest edge of the ice floe field of concentration CT = 78% on AARI map resembling the shape of the Edge-2 was found at a distance of 4 Nm in the direction of 014°. The Edge-3 field generally corresponded to the position of ice floe field of concentration CT = 13% situated at a distance of 1-5 Nm in the direction of 090°. It was assumed that there was moderate harmony of data.

The aari_bar_20090818_pl_a (SHP, SHX, DBF, PRJ) file was used for comparison with the observed from the vessel edge of ice floe field Edge-4. It was assumed that the map represented ice conditions dated 2009.08.17 12:00 UTC because it reflected the average ice cover for the last three days. The time difference was 2.56 days. The closest edge of the ice floe field (CT = 91%) was offset, in relation to the edge of the ice edge of concentration 25-60% observed from the vessel (Edge-4) at a distance 27 Nm in the direction of 312 °. It was assumed, therefore, that there was no relationship between these data. Mean offset position with respect to the edge of the ice floe that was observed from the vessel was 10 Nautical miles.

5.1.4 *The IUP maps of ice floe concentration in raster GeoTIFF format*

The asi-n3125-20090810.TIF file was used for comparison with the observed from the vessel ice floe field edges dated respectively Edge-1 (2009.08.10 12:00 UTC), Edge-2 (2009.08.10 13:25 UTC) and Edge-3 (2009.08.10 15 45 UTC. It was noted that the GeoTIFF map was offset from the edges of the ice fields and land masks 6 Nm in the direction of 120°. It was found out that, after taking this offset into account, the nearest edge of the field of concentration CT = 10% on GeoTIFF map was coincident with the shape of the Edge-1 located at a distance of 17 Nm in the direction of 350° and was coincident with the shape of the Edge-2 at a distance of 23 Nm in the direction of 346°. At the same time the edge of ice floe field of concentration CT = 20-40% consistent with the shape of the Edge-3 was lying at a distance of 4 Nm in the direction of 065°. Thus configuration of the ice fields edge on the IUP map was distinctive and consistent with the edges of the ice floe seen from the vessel but at relatively large distance.

The asi-n3125-20090815.TIF file was used for comparison with the observed from the vessel ice floe field Edge-4 dated 2009.08.15 10:43 UTC. It was noted that this GeoTIFF map was offset from the edges of

the ice field and land mask 6 Nm in the direction of 120°. It was found out that, after taking this offset into account, the nearest edge of the field of concentration CT = 20% on GeoTIFF map was coincident with the shape of the Edge-4 located at a distance of 34 Nm in the direction of 013°. Configuration of the ice floe edge on IUP map is not very clear.

5.1.5 *The NIC maps of the ice concentration in a MIZ scale in vector Shapefile format*

The nic_miz2009222nc_pl_a.zip (SHP, SHX, DBF, PRJ) file dated 2009.08.10 was used for comparison with the observed from the vessel ice floe field edges dated respectively Edge-1 (2009.08.10 12:00 UTC), Edge-2 (2009.08.10 13:25 UTC) and Edge-3 (2009.08.10 15 45 UTC. The ice floe field Edge-1 was located like border CT = 18-81% presented by MIZ file. This limit was also the beginning of the route in the area covered by ice. The MIZ wedge of a high concentration of ice floe shown on NIC map was offset 4 Nm in the direction of 028° with respect to Edge-2. Field of Edge-3 was found to be entirely located in the area of CT = 18-81%concentration as shown by the MIZ map. It was assumed that data were in general harmony.

The nic_miz2009227nc_pl_a (SHP, SHX, DBF, PRJ) file dated 2009.08.15 was used for comparison with the observed from the vessel ice floe field Edge-4 dated 2009.08.15 10:43 UTC. The nearest edge of ice (CT = 18-81%) on NIC map passed exactly through the area of the observed Edge-4field. Instead of the expected wedge with a higher concentration of ice extended to the South this map showed the general ice limit on NW-SE direction. This was consistent with the observed field of low ice floe concentration on the route from Kinnvika to the area of Edge-4 (see Table 3). The closest edge of ice floe field of CT > 81% concentration was offset from the observed edge of ice of 25-60% concentration (Edge-4) 20 Nm in the direction of 000°. It might be assumed that there was a general correlation between data. However, it was low in detail due to the different edges concentration presented on map nic_miz2009227nc_pl_a and the edge observed from the vessel.

5.1.6 *The NCEP maps of ice concentration in gridded GRIB format in a resolution of 5 minutes of arc*

The ice5min.200908.grb file for the date 2009.08.10 was used for comparison with the observed from the vessel ice floe field edges dated respectively Edge-1 (2009.08.10 12:00 UTC), Edge-2 (2009.08.10 13:25 UTC) and Edge-3 (2009.08.10 15 45 UTC. Field of ice floe Edge-1 was situated in the area of 40-50% concentration; Edge-2 in the area of 0-5% concentration, Edge-3 was located in the area of 0-40% shown on GRIB map. Data consistency is correct for Edge-1 and Edge-3. However, the lack of continuity presented by the GRIB map raised concern that the results of the comparison may be largely random. I was assumed that there was only very general harmony of data.

The ice5min.200908.grb file for the date 2009.08.15 was used for comparison with the observed from the vessel ice floe field Edge-4. The closest corresponding to the shape of the edge of ice floe concentration field CT = 25-35% was offset from the vessel observed 25-60% ice edge (Edge-4) 8 Nm in the direction of 013°. It might be assumed that there was a general consistency between data. However, it was low in detail due to the different concentration edges being on map ice5min.2009-08.grb and the edge observed from the vessel.

5.1.7 *The IFREMER ice concentration maps in gridded NetCDF format without geographical coordinates*

The 20090810.nc file was used for comparison with the observed from the vessel ice floe field edges dated respectively Edge-1 (2009.08.10 12:00 UTC), Edge-2 (2009.08.10 13:25 UTC) and Edge-3 (2009.08.10 15 45 UTC. Field of ice floe Edge-1 was in the area of 0-11% concentration, Edge-2 in the area of 11-22% concentration, Edge-3 was in the area of 11-44% visualised by NetCDF map. Thus it has been assumed that this grid map does not recognize the local significant changes in ice floe concentration.

The 20090815.nc file was used for comparison with the observed from the vessel ice floe field Edge-4 dated 2009.08.14 22:30. The closest NetCDF map area of the CT = 22-44% concentration corresponding to the shape of the ice floe edge observed from the vessel 25-60% (Edge-4) was offset 32 Nm in the direction of 354°. It might be assumed that there was a general consistency between data. However, it was low in detail due to different concentration edges being on map 20090815.nc and the edge observed from the vessel.

5.1.8 *The NIC maps of sea ice extent and sea ice limit in vector Shapefile format*

The masie_ice_r00_v01_2009222_4km.ZIP (SHP, SHX, DBF, PRJ) file dated 2009.08.10 was used for comparison with the observed from the vessel ice floe field edges dated respectively Edge-1 (2009.08.10 12:00 UTC), Edge-2 (2009.08.10 13:25 UTC) and Edge-3 (2009.08.10 15 45 UTC. The shape of MASIE line was not correlated with the observed from the vessel ice floe edges. The closest corresponding to the MASIE line of ice floe CT> 40% concentration is located with respect to the observed from the vessel 25-60% ice edge (Edge-1) at a distance of 25 Nm in the direction of 003°. It might be assumed that there is no correlation between the data.

The masie_ice_r00_v01_2009227_4km (SHP, SHX, DBF, PRJ) file dated 2009.08.15 was used for comparison with the observed from the vessel ice floe field Edge-4. The closest MASIE line of CT > 40% corresponding to the observed ice edge (Edge-4) of 25-60% concentration was offset 28 Nm in the direction of 354°. It might be assumed that there was a general consistency between data. However, it was low in detail due to the different concentrations of edge provided by the MASIE map and ice floe edge observed from the vessel.

5.1.9 *The OSISAF ice concentration and ice type maps in gridded NetCDF format with geographical coordinates*

The ice_conc_nh_YYYYMMDDHHMM.nc, ice_edge_nh_YYYYMMDDHHMM.nc and ice_-

type_nh_YYYYMMDDHHMM.nc file were used for comparison with the observed from the vessel ice floe field Edge-4 dated 2009.08.14 22:30. The closest ice_conc_nh_YYYYMMDDHHMM.nc map area of the CT = 0% concentration corresponding to the shape of the ice floe edge observed from the vessel 25-60% (Edge-4) was offset 10 Nm in the direction of 300°. It might be assumed that there was a general consistency between data. However, it was low in detail. Thus it has been assumed that this grid map recognize generally the local significant changes in ice floe concentration.

The closest ice_edge_nh_YYYYMMDDHH-MM.nc map area of the CT = 40% concentration corresponding to the line of the ice floe edge observed from the vessel 25-60% (Edge-4) was offset 23 Nm in the direction of 330° and the CT = 70% concentration corresponding to the same was offset 32 Nm in the direction 330°. Thus it has been assumed that these two grid maps do not recognize the local significant changes in ice floe concentration.

The closest ice_type_nh_YYYYMMDDHH-MM.nc map area of the ambiguous type (Open Water side) corresponding to the line of the ice floe edge observed from the vessel 25-60% (Edge-4) was offset 19 Nm in the direction of 330°. This edge does not recognise the local significant changes in ice floe concentration. Same time the ambiguous type (First year ice side) corresponding to the line of the ice floe edge observed from the vessel 25-60% (Edge-4) was offset 25 Nm in the direction of 315°. This ambiguous edge shape corresponded generally to the shape of Edge-4. Thus it has been assumed that these ambiguous edges recognize generally the local significant changes in ice floe concentration.

Need to remember that following visual observations from the vessel the sea ice floe thickness was estimated to be equal from 36 to 72 cm with inclusions of hummocked ice floe 180 cm high and only in exceptional cases the hummocked ice floe was 288 cm. Following these observations was assumed that the higher ice floe thickness at the centre of analysed ice floe fields and in the ice floe fields far away North from the route of the vessel were shown on OSISAF ice age map. This map not recognized sea ice floe of lower thickness especially of smaller coverage then cell size and lower concentration then 70%. The land filter also was the limitation.

5.1.10 *The NSIDC-CCAR ice age maps in raster GIF format without geographical coordinates*

The age2009_33.gif file was used for comparison with the observed from the vessel ice floe field Edge-4 dated 2009.08.14 22:30. The closest age2009_33.gif map area of age data corresponding to the shape of the ice floe edge observed from the vessel 25-60% (Edge-4) was offset 12 Nm in the direction of 315°. It might be assumed that there was a general consistency between data. However, it was low in detail. Thus it has been assumed that this grid map recognize generally the local significant changes in ice floe concentration.

The NSIDC-CCAR ice age map shown high volatility of course and general similarity of the edge patterns with other maps or observations form the vessel in two locations around position 80°N / 009°E and 80°N / 015°E along 160 Nm of analysed sea ice limit. The 1st and 2nd year ice age along this pattern represented mean thickness of ice 149 cm and 202 cm respectively. Following visual observations from the vessel the sea ice floe thickness (high) was estimated equal from 36 to 72 cm with inclusions of hummocked ice floe 180 cm high and only in exceptional cases reaching 288 cm high. Following these observations was assumed that the higher ice floe freeboard at the centre of analysed ice floe fields and in the ice floe fields far away North from the route of the vessel are shown on NSIDC-CCAR map. This map not recognized sea ice floe of lower thickness especially of smaller coverage then cell size and lower concentration then 70%. The land filter also was the limitation.

5.2 *Verification of ice data presented by NIS remote sensing source maps named c_map3*

The first, the content of the NIC map named barnwYYMMDDcolor and NIS map named c_map3 was compared. The analysis included offset of ice edge position on the NIC map barnwYYMMDDcolor described in section 5.1.1. A 30-50% concentration boundary on the map barnwYYMMDDcolor was consistent with the edge of 40-70% concentration on c_map3 map. The concentration limits of 70-90% and 90-100% on the map c_map3 coincided with 50-70% edge on barnwYYMMDDcolor map and 90% edge on barnwYYMMDDcolor map where the edge of 50-70% was not shown on the map.

The edge of the concentration of 81% on the NIC map named nic_mizYYYYDDDnc_pl_a reflected approximately 40% concentration edge on the NIS map named c_map3. The limit concentration of 18% on the map nic_mizYYYYDDDnc_pl_a reflected approximately 0-10% concentration edge on the map c_map3.

The edge of the ice concentration of 90 (91) % on the AARI map named aari_bar_20090818_pl_a clearly reflected the edge of the concentration of 90% on NIS map named c_map3. Fields with a concentration of 13-78% on the aari_bar_200908-18_pl_a map reflected 10-40% and 40-90% concentration field on the map c_map3. Field of concentration of 40-70% on the map c_map3 was lying inside the field of concentration of 46-78% on the map aari_bar_20090818_pl_a. Fields with a concentration of 78-90% on the map aari_bar_20090818_pl_a reflected field of concentration of 40-70% on the map c_map3. The edges of the ice concentration of 0% were consistent on both maps. The edge of the ice concentration of 40% on the NIC map named masie_ice_r00_v01_2009227_4km mostly reflected the edge of the concentration of 40% on NIS map named c_map3.

5.2.1 *NIC maps named barnwYYMMDDcolor*

The analysis included offset of ice edge position on the NIC map named barnwYYMMDDcolor described in section 5.1..2. The edge of the ice concentration of 81% on the NIC map named nic_mizYYYYDDDnc_pl_a was consistent with the

edge of 50-70% and 90% on the map barnwYYMMDDcolor where the edge of the concentration of 50-70% was not shown on the map barnwYYMMDDcolor. The edge of the concentration of 18% on the map nic_mizYYYYDDDnc_pl_a coincided with the edge of the concentration of 50-70% on the map barnwYYMMDDcolor. In this case, the edge of 50-70% was the limit of data related to sea ice.

Fields with a concentration of 46% and 78% from the lower limit of the field edge and concentration of 90% as the upper limit on aari_bar_20090818_pl_a maps were consistent with the edge of concentration of 90% on the map barnwYYMMDDcolor. The edge of the ice coverage (concentration of 0%) on the map barnwYYMMDDcolor North of the Nordaustlandet Island was the same as on the map aari_bar_YYYYMMDD_pl_a but the edge of 0% on the North and Northwest of Svalbard on the map barnwYYMMDDcolor was located more to the South and contained more details than aari_bar_YYYYMMDD_pl_a map.

The edge of ice concentration of 40% on the NIC map named masie_ice_r00_v01-_2009227_4km roughly coincided with the edge of 30-50% on the NIC map named barnwYYMMDDcolor. Just like in the case of AARImaps, the edge of the ice concentration of 30-50% on the map barnwYYMMDDcolor was located more to the South than on the map masie_ice_r00_v01_2009227_4km. It also contained more details than MASIE map.

5.2.2 *IFREMER maps named YYYYMMDD*

The fields with the specified concentration on the IFREMER map represented fairly the ice concentration field on the NIS map named c_map3. The limitation was the relative large size of the grid (cell) on IFREMER map. Similar difficulties for comparison were due to lack of information in the fields appearing on the IFREMER map.

The edge of the ice concentration of 81% on the NIC map named nic_mizYYYYDDDnc_pl_a approximately reflected the distribution of concentration fields of 44-78% on the IFREMER maps named YYYYMMDD.nc. However, the edge of the ice on the NIC maps ran parallel through the fields with smaller values of concentration of IFREMER maps.

The edge of the concentration of 78 (90)% on the AARI maps named aari_bar_YYYYMMDD_pl_a reflected 78% concentration field on the IFREMER map named YYYYMMDD.nc. The edge of the concentration of 13% on the AARI maps reflected fields of the concentration of 33% on the IFREMER map.

The edge of the ice concentration of 40% on the NIC map named masie_ice_r00_v01_2009227_4km runs through or near the fields of concentration of 44-56% on the IFREMER maps. The spatial distribution of these edges was very consistent.

5.2.3 *NCEP maps named ice5min.YYYYMM*

The edge of the concentration of 81% on the NIC maps named nic_mizYYYYDDDnc_pl_a generally ran along the edge of the concentration of 40% on the NCEP map named ice5min.YYYYMM. There were discrepancies. The edge of the ice on the nic_mizYYYYDDDnc_pl_a map ran through the lower concentration values on the NCEP map. The edge of the concentration of 18% on the nic_mizYYYYDDDnc_pl_a maps generally ran along the edge of the concentration of 0-20% on the ice5min.YYYYMM map but there was derogation. The fields on both maps were consistent.

The edge of the concentration of 90% on the AARI map named aari_bar_YYYYMMDD_pl_a mostly ran through the fields of concentration of 70-80% on the map ice5min.YYYYMM but there was derogation. The edge of the ice concentration below 13% on the AARI map edge reflected approximately edge of 20% concentration on the NCEP map. The edges of the concentration of 46% and 78% on the AARI map reflected data on the NCEP map only in a very general way.

The edge of 40% concentration on the NIC map named masie_ice_r00_v01_2009227_4km mostly ran through the fields of concentration of 40% on the ice5min.YYYYMM map. There was derogation. In such cases, the NCEP map showed mostly lower concentration values than MASIE map.

Fields with 85% concentration on the NCEP map named ice5min.YYYYMM quite accurately reflected edge of 90% concentration on NIS map named c_map3. The edge of the concentration 70% on the NCEP map was less coincident with the field of 50-70% concentration on NIS map. The limit of ice 0% concentration on the NCEP map corresponded roughly the edge of concentration of 0-10% on NIS map.

5.2.4 *IUP maps named asi-n3125-YYYYMMDD*

The edge of 40% concentration on NIS map named c_map3 reflected roughly the fields of concentration 20% or 70-80% on the IUP map. It was noted that the edge of 0% concentration on the IUP map corresponded to the edge of the 40% concentration on the NIS map. The higher the concentration, the smaller is discrepancy of position for each ice floe concentration.

The edge of 81% concentration on the NIC map named nic_mizYYYYDDDnc_pl_a accurately reflected edge of 0% concentration on the IUP map named asi-n3125-YYYYMMDD.

The edge of 90 (91) % concentration on the AARI map named aari_bar_YYYYMMDD_pl_a accurately reflected fields of 80-90% concentration on the IUP map. The edge of 78% concentration on the AARI map accurately reflected 10-20% concentration field on the IUP map.

The edge of 13-46% concentration on the AARI map took place in areas of 0% concentration on the IUP map. The edge of 40% concentration on the NIC map named masie_ice_r00_v01_2009227_4km mostly reflected edge of concentration of 0-10% on the IUP map.

5.2.5 *OSISAF ice concentration maps named ice_conc_nh_YYYYMMDDHHMM*

The limit of concentration 0% on the OSISAF maps named ice_conc_nh_YYYYMMDDHHMM reflected very roughly Open Water (10%) limit marked on NIS map named c_map3. Maximal discrepancies of characteristic limits location reached up to 16 Nm in both directions (North or South). Ice limits of concentration 0% on OSISAF map were located on the average distance 6 Nm North from Open Water (10%) limit on NIS map at a standard deviation error around 12 Nm. There was found that the OSISAF concentration map not identified ice fields up to 5 Nm wide nor rectangles of ice fields of 10-70% concentration up to 12-24 sq. Nm marked on NIS map.

The 40% concentration limit on the OSISAF ice_conc_nh_YYYYMMDDHHMM map very roughly corresponded to center of 40-70% concentration field marked on NIS c_map3 map. The 40% concentration limit on the OSISAF map was offset average 8 Nm South from c_map3 40-70% field with a standard deviation error 5 Nm. The OSISAF ice_conc_nh_YYYYMMDDHHMM map not identified ice fields up to 5 Nm wide nor rectangles of ice fields of 40-70% concentration up to 15-46 sq. Nm marked on c_map3 map.

The 40% concentration limit on OSISAF ice_conc_nh_YYYYMMDDHHMM map was offset average 5 Nm North from 40-50% concentration limit on barnwYYMMDDcolor map with a standard deviation error 7 Nm.

The 40% concentration limit on OSISAF ice_conc_nh_YYYYMMDDHHMM map not identified 40-50% concentration ice fields up to 14 Nm wide nor rectangles of ice fields of 40-50% concentration up to 150 sq. Nm on the NIC barnwYYMMDDcolor map.

5.2.6 *OSISAF ice concentration maps in simplified scale named ice_edge_nh_YYYYMM-DDHH-MM*

Spatial distribution of 70% concentration limit on the OSISAF maps named ice_edge_nh_YYYY-MMDDHHMM was consistent with the trends of 40% ice concentration limit on the IUP map named asi-n3125-YYYYMMDD but 40% concentration limit on the IUP map ran more to the North in relation to 70% concentration limit presented on the OSISAF ice_edge_nh_YYYYMMDDHHMM map about 7 Nm. Spatial distribution of 40% concentration limit on the IUP map was significantly much more volatile than 70% concentration limit on OSISAF ice_edge_nh_YYYYMMDDHHMM map.

The course of 70% concentration limit on the OSISAF ice_edge_nh_YYYYMMDDHHMM map was also coincident with 40% concentration limit on the NCEP map but 70% concentration limit on the OSISAF ice_edge_nh_YYYYMMDDHHMM ran on the average distance 2 Nm more to the North than 40% concentration limit on the NCEP map. This relationship seemed quite properly took into account average real distribution of ice concentrations.

The 70% ice concentration limit on OSISAF map named ice_edge_nh_YYYYMMDDHHMM ran similarly with 81% ice concentration limit presented on the NIC MIZ map named nic_miz2009-222nc_pl_a and also a little better with 46% (or 91%) concentration limit presented on the AARI map named aari_bar_YYYYMMDD_pl_a limit beginning NW of Svalbard up to Nordaustlandet Island.

The 70% concentration limit on OSISAF ice_edge_nh_YYYYMMDDHHMM map ran generally same way like 40% concentration limit on NIC MASIE. Standard deviation error of both limits locations was equal 5 Nm.

The 70% concentration limit on OSISAF ice_edge_nh_YYYYMMDDHHMM map ran average 2 Nm South in relation to 70% concentration limit placed on NIS c_map3 map with a standard deviation error equal 4 Nm.

The 70% concentration limit on OSISAF ice_edge_nh_YYYYMMDDHHMM map ran aver-age 7 Nm South in relation to 70-90% concentration limit on the NIC map named barnwYYMMDDcolor with a standard deviation error 6 Nm.

5.2.7 *OSISAF ice age maps named ice_type-_nh_YYYYMMDDHHMM*

The 70% concentration limit on the OSISAF ice_edge_nh_YYYYMMDDHHMM map coincided with the „ambiguous" edge of ice (from Open Water side) on OSISAF ice_type_nh_YYYYMMDD-HHMM map almost in its entirety a few minor variations in both directions.

The 40% concentration limit on the OSISAF ice_conc_nh_YYYYMMDDHHMM ran mostly in the middle of the „ambiguous" zone of the OSISAF ice_type_nh_YYYYMMDDHHMM map (from Open Water limit till 1st year ice limit).

The limit of ice covered area on NSIDC-CCAR map named ageYYYY_WW coincided relatively well with limit of the „ambiguous" zone of the OSISAF ice_type_nh_YYYYMMDDHHMM map (from 1st year ice limit). Both maps identified

5.2.8 *NSIDC-CCAR ice age maps named age-YYYY_WW*

The limit of ice covered area on NSIDC-CCAR map named ageYYYY_WW coincided mostly with 0% concentration limit on OSISAF ice_conc_nh_-YYYYMMDDHHMM map. However, there were derogation. Trends of both lines were consistent over the entire length of examined lines from the western part of North Svalbard to the western edge of Nordaustlandet Island despite significant standard deviation error of 8 Nm. The average deviation of the position of each line was null. This meant that averaged lines completely overlapped.

The edge of ice age data on NSIDC-CCAR ageYYYY_WW map reflected relatively well the 40% ice concentration limit pattern placed on NIS c_map3 map. The NSIDC-CCAR ice age data limit was offset average 13 Nm South in relation to c_map3 40% concentration on NIS c_map3 limit with a standard deviation 5 Nm. The NSIDC-CCAR map not identified 40-70% concentration ice fields up to 5 Nm wide nor rectangles of ice fields up to 25 sq. Nm on OSISAF ice_conc_nh_YYYYMMDD-HHMM map.

The edge of ice age data marked on NSIDC-CCAR map reflected relatively well 40-50% concentration limit being on NIC map named barnwYYMMDDcolor. The NSIDC-CCAR ice age data limit was offset average 10 Nm South in relation to 40-50% concentration on NIC barnwYYMMDDcolor map with a standard deviation 6 Nm. Ice edge features being on NIC barnwYYMMDDcolor map ran same to those of NSIDC-CCAR ice edge that were offset on approximate direction 160°.

5.3 *Spatial distribution of analysed lines*

The next examination was related to the spatial distribution of individual lines in the studied region for the 15th August 2009. There was analyzed the distribution of isolines from the first boundary of sea ice occurrence up to the line with the highest concentration of ice in the range from 70 to 91 % of ice floe concentration. These lines were lying in general direction 050° - 230°. Some of them did not show extraordinary variation from this general direction. The only lines of NIS maps named c_map3, NIC maps named barnwYYMMDDcolor and IUP maps named asi-n3125-YYYYMMDD shown a very diverse course. Nearly all data sources shown high volatility of course only in two locations around position 80°N / 009°E and 80°N / 015°E along 160 Nm of analysed sea ice edge. One of them was identified by observations from the vessel.

The mean value of standard deviations of all lines shown in Figure DDD was equal 8.3 Nm irrespective of the distance from the beginning of ice. The standard deviation of these mean values was equal 0.85 Nm. Assumed it was very small value. In step 6 (Figure DDD) occurred anomaly associated with high volatility of course in locations around position 80°N / 009°E. The convexity of the ice field boundary was demonstrated well by the NSIDC-CCAR map (19 Nm), then the NIC MIZ map (11 Nm) and NIS c_map3 map (7 Nm). In step 12-13 (Figure DDD) occurred anomaly associated with high volatility of course in locations around position 80°N / 015°E. The convexity of the ice field boundary was demonstrated well by the NIC barnwYYMMDDcolor (29 Nm), then the NIC MIZ map (24 Nm) and NIS c_map3 map (24 Nm). The line of NSIDC-CCAR (figure DDD) shown no clear correlation with changes in the course with other boundary lines. The most distant from the ice edge line was 40% concentration line shown on IUP map. It reached mostly further to the North than the lines of high 70-81-91% concentration. Due to this significant derogation from the other lines, the IUP line was not taken into account in the following analysis. It is worth mentioning that another far away from beginning of sea ice was 40% concentration line shown on NIC MASIE map and next was 40% concentration line shown on NCEP map.

Interesting looks correlation of same kind of edges in relation to the distance from the beginning of sea ice field. Average distance of center of "ambiguous" zone presented on OSISAF ice age maps was equal 21 Nm. Average distance of all analysed lines representing 30-40% ice floe concentration (IUP product excluded) was equal 24.1 Nm, Average distance of all analysed lines representing 70-81-91% ice floe concentration was equal 30.6 Nm. The maximum average value of distance of the furthest analysed line (IUP product excluded) was equal 37.2 Nm. The average standard deviation of that averages was equal 8.3 Nm only. It is worth mentioning that tendencies of distance changes were very well correlated (Figure 6).

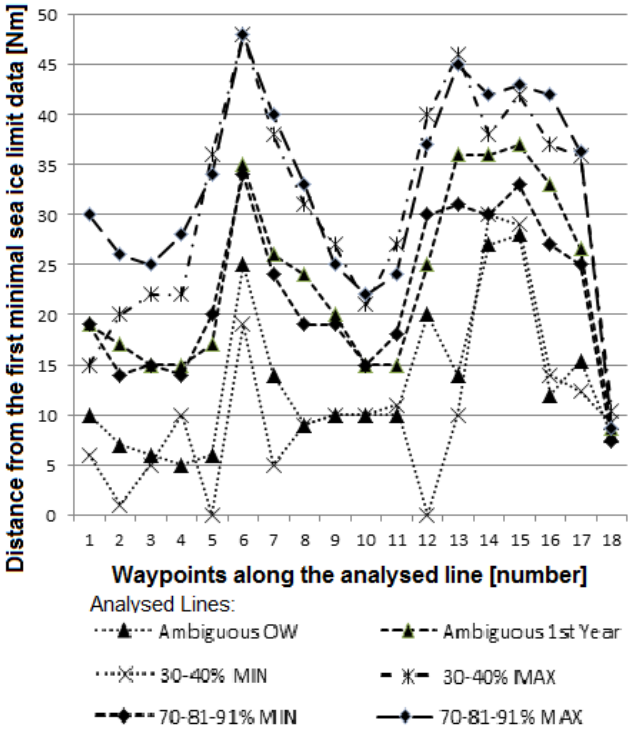

Figure 6. Distance of selected edges from the first minimal sea ice limit data along general direction of ice limit.

Also interesting looks correlation of maximal distances in the groups of same kind of edges in relation to the distance from the beginning of sea ice field. Distance of "ambiguous" zone edge presented on OSISAF ice age maps from Open Water side was equal 15.4 Nm. Distance of "ambiguous" zone edge presented on OSISAF ice age maps from 1st year ice side was equal 26.6 Nm. Maximal distance of any line from lines representing 30-40% ice floe concentration (IUP product excluded) was equal 35.9 Nm, Maximal distance of any analysed line from lines representing 70-81-91% ice floe concentration product excluded) was nearly same like 30-40% and equal 36.3 Nm. The maximum value of distance of the furthest analysed line (IUP product excluded) was equal 37.2 Nm. The average standard deviation of that averages was equal 8.3 Nm only. It is worth mentioning that tendencies of distance changes were very well correlated (Figure 6). The minimal distance of any analysed line from lines representing 70-81-91% ice floe concentration (IUP product excluded) was equal 25 Nm. This line was also very well correlated with all above mentioned edges. The minimal distance of any analysed line from lines representing 30-40% ice floe concentration (IUP product excluded) was equal 12.3 Nm but this line was not so well correlated with other above mentioned edges.

6 EVALUATION OF USEFULNESS OF REMOTE SENSING DATA FOR ROUTEING PURPOSES

NIS maps named c_map.jpg accurately reflected the edges of the ice floes field observed from the vessel at the moment of reference. Mean offset position was 3.7 Nm. The ice floe patches of a width of less than 1.0 Nm were not detected by remote sensing. Also NIC map named barnwYYMMDDcolor accurately reflected condition of the ice cover observed from the ship at the moment of reference. It was assumed that wedge of ice field of a width of less than 1.5 Nm was not detected by remote sensing. Based on observations made from the vessel, the two maps seemed to be appropriate for voyage planning and routeing of the vessel in ice for every ice class vessel (see section 4). It is also possible to optimize the routeing using these maps in accordance with the criteria specified by Kjerstad (2011), Arikaynen and Tsubakov (1987) and CCG (1992). It is routeing of the vessel along the lightest ice conditions.

NIC maps named nic_mizYYYYMMDDnc_pl_a show general compliance with the shapes of the edge of the ice fields observed on the vessel. Mean offset position for the characteristic shapes of the edge of the ice fields was 6.5 Nm. AARI maps named aari_bar_YYYYMMDD_pl_a seemed to be highly generalized and did not reflected the state of the ice cover observed from the vessel. Mean offset position for the characteristic shapes of the edge of the ice fields was 5.8 Nm. It was assumed that ice field of a width less than 5 Nm remained undetected by remote sensing. Both of these maps showed a consistent location of MIZ lower limit of 0-18% and MIZ upper limit of 70-90% visualised on the maps c_map3 and NIC NIS barnwYYMMDDcolor. Despite greater number of concentration levels provided by the AARI map, AARI map seemed to be less precise in detail than the NIC MIZ map. Due to the limitation of the precision of the scale of concentration or precision of position, the above maps seemed to be useful for the preliminary voyage planning and routeing of the vessel. They were not useful for optimizing the routeing of the vessel in accordance with the criteria specified by Kjerstad (2011), Arikaynen and Tsubakov (1987) and CCG (1992).

NCEP maps named ice5min.YYYYMM showed general consistency between the data. It was assumed that the average position offset of ice fields shapes corresponded to the dimensions of the grid of 9.4 Nm. However, lack of continuity (consistency) of the data on the NCEP map was noted. This raised concerns that the concentration field visualized by the map may not accurately reflect the actual ice conditions in a particular place and thus lead to an incorrect assessment of navigational situation or prevent proper determination the routeing of the vessel.

NIC maps named masie_ice_r00_v01_2009-222_4km were related to ice floe concentration of 40%. Average offset of ice field shapes on MASIE map in relation to ice fields observed from the vessel was 20.6 Nm. IFREMER maps named YYYYMMDD showed a slight similarity with the observations of ice cover made from the vessel, with NIC maps barnwYYMMDDcolor and NIS c_map3 maps. However, the shape of the edge of the ice floe field of concentration above 11% on IFREMER map most closely corresponded to the shape of ice edge on the IUP map. It was assumed that the average position offset of the characteristic shapes of ice edge fields was as much as a side of the grid (cell) of IFREMER map equal to 6.7 Nm. IUP maps named asi-n3125-YYYYMMDD showed average position offset of the ice field shapes equal to 19.5 Nm. Therefore it was assumed that the fields of ice floe on IUP map did not reflected directly the ice edge observed from the vessel. The edge of 0-10% concentration on the IUP map corresponded to the edge of concentration of 40% on c_map3 NIS map, to the edge of concentration of 30-50% on NIC barnwYYMMDDcolor map, to the edge of concentration of 40% on NIC MASIE map, to the edge of concentration of 81% on the NIC nic_mizYYYYDDD-nc_pl_a map, to the edge of concentration of 13-46% on the AARI aari_bar_YYYYMMDD_pl_a map and to edge of concentration of 11-44% on the IFREMER map. It was assumed that the NIC MASIE maps and ice limits on the IFREMER and IUP maps reflect the concentration limits of the ice floe of 30-40% due to the weather filters applied. Full scale of ice concentration on both of the above mentioned maps may be misleading. All three maps cannot be used for routeing of the lowest ice class vessels in the ice or in the vicinity of ice. However, they appear to be useful for vessels of the lowest classes of ice (see Table 1) as they indicate the limits of the region with average 30-40% concentration of ice floe. These vessels can navigate in this area with icebreaker assistance. The use of IFREMER and IUP maps for vessels with higher ice classes routing does not seem to be appropriate because they do not reflect the real concentration of ice floe.

7 EVALUATION OF USEFULNESS OF REMOTE SENSING DATA FOR VESSEL'S SPEED ESTIMATION

Accuracy of scale of sea ice concentration and ice thickness, which were used in analyzed data sources, is important for estimation of vessel's maximum safe speed. It is difficult to compare the quality of scales of individual sources.

It was found that scales of data sources are discrete of various steps: NIS – irregular steps 0-10, 10-40, 40-70, 70-90 and 90-100 %, NIC (barnw) - variable steps 10-30, 20-40, 30-50, 40-60, 50-70, 60-80, 70-90, 80-100 and 90-100 %, AARI – few steps only of 13, 46, 78, 91%, NIC (MIZ) – large steps for 18% and 81% only, NCEP – 0.5%, OSISAF (concentration) – continuous scale but in practice discrete one at 0.1% concentration and after taking into account weather filter 35% concentration, IFREMER (concentration) – continuous scale but in practice discrete one at 0.1% concentration and after taking into account weather filter 15% concentration, IUP - 0.5% step after taking into account the weather filter 40% concentration of ice floes, OSISAF (simplified concentration scale) – only few steps of 0, 35 and 70% after taking into account weather filter of 35% concentration, NIC (MASIE) – only one edge but after taking into account weather filter of 40% concentration and being the result of summary of many various data sources, OSISAF (ice type/age) – few steps only like uncertain (ambiguous),

1st year, uncertain (ambiguous), multiyear ice, NSIDC-CCAR – few steps only like 1st year, uncertain (ambiguous), 2nd year and so on.

It should be emphasized that ESIMO distinguished following intervals of young ice thickness: Nilas (<10 cm), gray (10-15 cm) and a gray-white (15-30 cm). First-year ice was divided into thin (30-70 cm), medium (70-120 cm) and thick (120-200 cm). First-year ice is sea ice that has not survived more than one winter. It was also assumed that multiyear ice (old) has a thickness of 200 cm and more. The applied scale seems to be a detailed and satisfying the needs of assessment of a safe speed of the vessel in ice based on Arikaynen (1979) criteria. However, it is not entirely consistent with the scale of the ice ages used by RMRS (2015).

Debatable issue is the interpretation of discrete scale on OSISAF ice type (age) maps. The scale contains edges of the 1st year ice and multiyear ice but the edge is determined by a complex filter that is reducing false ice and is adding the extent of ice cover up to 50 Nm following NSIDC ice extent from the day before. In this case the 1st year ice means current year young ice. The multiyear ice means that have survived at least one summer season (Eastwood 2014).

The discrete scale on NSIDC-CCAR ice age of every one year step represents mean thickness of ice equal 149 cm, 202 cm, 228 cm, 247 cm, 268 cm. In this case the first-year sea ice means "young" ice according to ESIMO classification or of the current winter or that not survived any melting season. It is equivalent of "current year young ice" according to OSISAF ice type scale. The second-year sea ice survived one melting season and so on. In this case the NSIDC-CCAR lowest value of ice thickness is related to high thickness around 149 cm that responding to medium and thick ice according to ESIMO scale. The NSIDC-CCAR scale looks like not containing equivalency of ice thickness from 0 to 70 cm of ice.

A separate issue is land filter used in the majority of analysed data sources. It limits much information near the shore and in the straits, archipelagos and narrow passages. Scales of ice ages do not reflect decay of ice. AARI changes maps from concentration type to thickness type and back on 1.VI and 30..IX . It suggest that decay of is substantial enough that makes ice thickness is not critical for safe speed of vessel. The provisions of RMRS (2015) apply additional criteria for the safe navigation of vessels of different ice classes in ice-covered areas. The possibility of completion of voyage depends on the area (of the sea) and the difficulties of ice conditions (extreme, hard, medium, easy).

The analysis of average speed of vessel of specified ice class in particular segments along the ice boundary found that relative standard deviation RSD of ice concentration was 34%. It was related to average concentration of all data sources along 180 Nm of distance. Were only two examined data sources related to ice thickness. NSIDC-CCAR data sources gave higher values of thickness than OSISAF data sources. Discrepancy of average ice thickness of both sources affected the high RSD. It was equal 92%. RSD of speed for both ice classes of vessels was higher in case of NSIDC-CCAR data than in case of OSISAF data. It was due to significantly greater variability in the direction of NSIDC-CCAR ice edge than in case of OSISAF data sources.

The reason seems to be the method of determining the ice edge on OSISAF map (see chapter 3.11). It was observed that the lower ice class of vessel, the higher speed deviation towards lower values (Table 5).

Local speed reduction occurred due to ice conditions may reach up to 32% of the average speed expected for ice class L1 and L3. Variations in velocity toward smaller values are more significant than can be seen from the calculated standard deviation (Tabela 5)

Table 5. Speed of defined ice class vessel in relation to average ice concentration and average ice thickness of data sources along the line of ice limit during voyage from Kinnvika to Longyearbyen following equation 2.

Data Source		30 Nm distance segments 1	2	3	4	5	6	Aver. RSD [kn]	[%]
Av.	CT [%]	45	15	33	38	41	52	37	34
Av.	H [cm]	15	0	15	116	90	116	59	92
NC-L3	V [kn]	5.8	6.0	6.0	3.8	4.0	2.8	4.7	29
NC-L3	σ [kn]	0.4	0.1	0.2	1.6	1.4	2.5	1.4	
NC-L1	V [kn]	11.6	12.1	12.0	7.7	7.9	5.7	9.5	29
NC-L1	σ [kn]	1.2	0.0	0.5	0.7	0.8	1.3	2.7	
OSI-L3	V [kn]	4.9	5.9	5.4	5.2	5.1	4.6	5.2	9
OSI-L3	σ [kn]	1.2	0.0	0.5	0.7	0.8	1.3	0.4	
OSI-L1	V [kn]	9.3	11.2	10.2	9.9	9.7	8.8	9.9	8
OSI-L1	σ [kn]	2.9	1.9	2.1	2.3	2.3	3.0	0.8	

NC- NSIDC-CCAR, OSI – OSISAF, CT – total concentration, H – ice thickness, σ – average, RSD – relative standard deviation

Mean concentration values for individual data sources were highly variable in the range between 0% and 77%. The average value for all sources was 37%. Relative standard deviation of average value of concentration for examined sources was equal 72% in relations to average concentration. The highest average values of vessel's speed of defined ice classes L3 and L1 are related to AARI, NCEP, IFREMER and IUP data sources. They were assumed to be too optimistic scenario. There were ice boundaries located the most Northward. This can be explained by the high value of weather filter equal 40% of ice concentration or because the information about ice occurrence begin at high concentration values above 40%. The lowest speed values fall on the OSISAF (EDGE) data sources. They were assumed too pessimistic scenario. This can be explained by high threshold of weather filter, high value of ice concentration limit on map and high step in between concentration thresholds of 35% and 70%. The intermediate speed values fall on NIS, NIC (barnw), NIC (MIZ), OSISAF (CONC) and NIC (MASIE) data sources. They were assumed most probable scenario.

Table 6. Average speed of defined ice class vessel in knots in relation to ice concentration and ice thickness for various data sources during voyage from Kinnvika to Longyearbyen following Equation 2.

Data Source	CT [%]	CCAR-L3 Av.	St.D.	CCAR-L1 Av.	St.D.	OSI-L3 Av.	St.D.	OSI-L1 Av.	St.D.
NIS	52	4.1	2.3	8.3	4.5	5.3	0.5	10.6	1.1
NIC	38	4.9	1.3	9.7	2.6	5.7	0.1	11.2	0.3

(barnw)									
AARI	0	5.8	0.1	11.6	0.3	6.1	0.1	12.1	0.2
NIC MIZ	77	3.3	2.7	6.5	5.4	4.9	0.5	4.9	0.5
NCEP	35	5.2	1.0	10.5	2.1	5.1	0.5	10.2	0.9
IFREMER	8	5.8	0.3	11.5	0.6	5.5	0.2	11.0	0.3
OSI CONC	51	4.2	2.1	8.5	4.2	4.5	0.8	9.1	1.7
IUP	0	5.8	0.1	11.6	0.3	6.1	0.1	12.1	0.2
MASIE	60	4.2	2.4	8.4	4.9	4.1	1.7	8.3	3.3
OSI EDGE	53	4.2	2.1	8.4	4.3	4.6	0.9	9.1	1.7
Aver. CT [%]	37	4.8	0.9	9.5	1.8	5.2	2.7	9.9	2.2
RSD [%]	72	18.0		18.0		13.0		22.0	

CT – total concentration, CCAR – NSIDC-CCAR, OSI – OSISAF, Av. – average speed [kn], St.D. – atandard deviation [kn], RSD – relative standard deviation [%]

Average speed of L3 ice class vessel ranged from 3.3 knots till 5.8 knots at average 4.8 knots for NSIDC-CCAR ice thickness data and from 4.1 knots till 6.1 knots at average 5.2 knots for OSISAF ice thickness data. Average speed of L1 ice class vessel ranged from 6.5 knots till 11.6 knots at average 9.5 knots for NSIDC-CCAR ice thickness data and from 4.9 knots till 12.1 knots at average 9.9 knots for OSISAF ice thickness data. Relative standard deviation of averaged speed for both ice class vessels was equal 18%. Higher volatility were found for OSISAF data sources. The highest relative deviations were found up to 50% below the average speed value. Same time the highest relative deviations were equal 22% above the average speed value.

Above mentioned relative deviations from average speed of the vessel are the result of discrepant data from the sources served for this evaluation. It means that the most important for evaluation of vessel's speed during voyage in ice-covered areas depends on data sources used for evaluation. That was assumed that the NIS, NIC (barnw), NIC (MIZ), OSISAF (CONC) i NIC (MASIE) data sources indicating most probable average values of speed should be good for low and medium ice class vessels for vessel's speed evaluation during voyage planning process. Distance in between points of beginning and end of the voyage with vessel speed corresponds with the time of the voyage.

Let's take above values into consideration for transit voyage planning on Northern Sea Route of total distance equal 3,032.8 Nm. The vessel of ice class L3 with average speed 5 knots require 50.5, 25.3 or 20.7 days for the voyage in pessimistic, most probable or optimistic scenarios respectively in case of extreme deviations were taken into consideration. The vessel of ice class L1 with average speed 9.7 knots require 26.1, 13.0 or 10.7 days for the voyage in pessimistic, most probable or optimistic scenario respectively in case extreme deviations were taken into consideration.

Average technical speed of "Norilsk SA-15" ULA class vessel was equal 12,6 knots (Mulherin 1996). It was assumed this speed corresponding well with speed of L1 and L3 ice class vessels estimated in this study. It means the appropriate assumptions have been adopted in the work. The standard deviation values may be used for voyage time planning instead of extreme relative deviation values. In any case a wide range of data sources and scenarios to be taken carefully into consideration.

8 CONCLUSIONS

The spatial range of whole analysed path of 0-90% concentration area covered by ice identified by various data sources was about 50 Nm (Figures 6 and 7). In case of 40% concentration data the spatial range was about 40 Nm. It can be related to distance passed by vessels with full sea speed 10-15 knots. Then this analysed zone was inside 2.5-5 hours of sailing in case of 0-90% concentration data and 2-4 hours of sailing in case of 40% concentration discrepancies only.

The results of analyses of different maps obtained by remote sensing methods showed that the information presented is not the same. An example of the edges and limits of the concentration of ice floe that are close to concentration of 40% for each map is shown in Figure 7. Discrepancies among the analysed data on the maps certainly arise from error of the measurement method. According to Rodrigues (2009) based on Comiso (1999) the error may be up to 5-10% and even 15% of the concentration of ice floe. This error depends on the remote sensing measurement method used. The error of the measurement method should be taken into account when planning the route of the vessel in ice-covered areas. It should also be borne in mind that the more generalized information about the state of the ice cover, the less likely becomes detection of ice floe patches of high concentration and theirs spatial extent. It should also be taken into account that the vessel may be trapped in the ice floe of a high concentration while overcoming larger ice floe field. Then icebreaker assistance will be required. In both these cases, the vessel will be able to sail at very low speed and thus lose a lot of time to go through the ice and the travel time becomes significantly longer. Thus, the current schedule and the next expedition schedule will be disrupted.

Now the question should be answered which maps may be used to assess the ice conditions from the navigation point of view. The MASIE, IFREMER and UIP maps seem to be useless for vessels with low ice class, as they relate to concentration of 30-40%. Such concentration edges might be useful for medium ice class ships. Low ice class vessels are looking for concentration limit of 15%. The NCEP maps also appear to be useless for low ice class vessels, because they may mislead the user during the preliminary voyage planning and scheduling the next expedition. The NIC (MIZ) and AARI maps seem to meet the needs of preliminary voyage planning and scheduling the next expedition of vessels with low ice classes as these maps depict the lower limits of 13-18% concentration. NIS maps named c_map3 and NIC maps named barnwYYMMDDcolor have a satisfactory scale concentration and precision to present the edge of each concentration. They allow planning the routeing of the vessel and avoiding areas with higher concentration of ice floe. When analysing the ice floe concentration on a map for planning the route and schedule of the vessel, the errors of remote sensing methods used to estimate concentration of ice floe should always be taken into consideration.

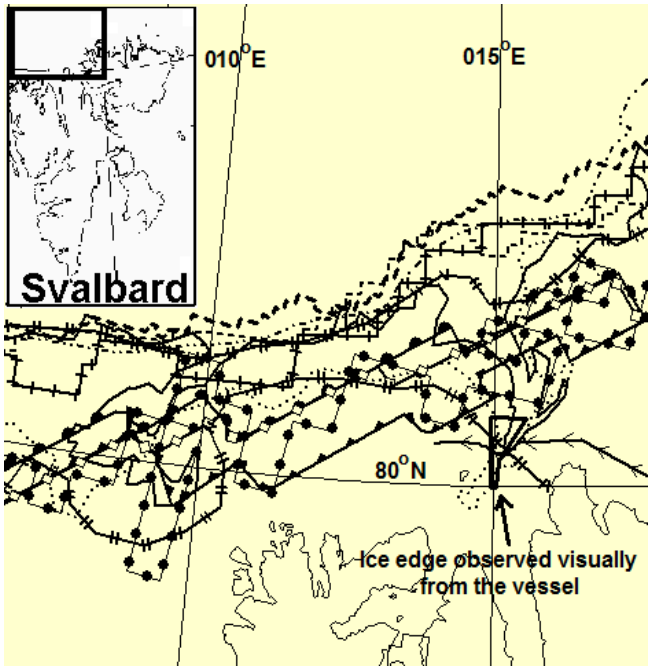

Figure 7. The spatial distribution of edges or borders close to 40% ice floe concentration for individual maps for the day 15 August 2009: —— edge of 40-70% concentration on the NIS map, • • • edge of 30-50% concentration on the NIC (EGG) map, — • • — edge of 46% or 91% concentration on the AARI map, — — — edge of 40% concentration on the NIC (MASIE), —┼— edge of concentration 40% on the NCEP map, —^— edge of 0% concentration on OSISAF map, —–— edge of 35% concentration on OSISAF ice edge map —●— ice edge on NSIDC-CCAR ice age map, —◊— ambiguous ice edge from Open Water side on OSISAF ice type map, —╫— edge of 0% or 81% concentration on NIC (MIZ) map, ——— edge of 25-65% concentration of ice floe field observed from the vessel. —◄— route of the vessel.

Finally, we must answer the question whether the above mentioned vessel of L2 (L1) class could determine more favourable route at an initial stage of routeing. The answer is positive. At the initial stage the crew could follow data on reliable daily NIS maps. The NIC barnwYYMMDDcolor maps were not available for required day. The NIC (MIZ) maps could be used but their content does not advise the vessel about higher concentration of ice patches. Thus the vessel probably would follow standard route to encounter ice floe patches of high concentration and make route around the ice field.

Another discussion require usefulness of analysed ice age maps for route planning. First, we should understand, that their scale is very generalised for ice thickness interpretation. Following the definition we can divide the scale of thickness of ice presented by these maps as young ice of thickness from 0 cm to 30 cm, first year ice of thickness from 30 to 200 cm and second year ice of thickness from 200 cm upwards.

The minimum ice floe concentration of 35% is identified by OSISAF ice type map. This is "area to be avoided" for vessels of ice class lower than L1 (Arikaynen 1987). OSISAF ice type maps are sensitive for melting period and wide stripe of ambiguous area is indicated instead of clear ice age data. This ambiguous area may be interpreted as area of younger ice then 1st ice age below 200 cm high and also as deteriorated ice of lower resistance and hardness, easier to overcome by vessel, despite considerable thickness. The location of edge in between ambiguous and open water area should be treated with caution because are determined by indirect remote sensing interpretation.

Ice edges courses included on NSIDC-CCAR ice age map are more reliable in details then OSISAF ice type map. The minimum ice floe concentration of 40% is identified by this map. This is "area to be avoided" for vessels of ice class lower than L1 (Arikaynen 1987). The user should expect ice thickness below 149 cm out of the ice fields. However this thickness is available for icebreakers and the highest ice class Arc7 (ULA) vessels only. The ice fields of any age shown on NSIDC-CCAR map should be interpreted as "areas to be avoided" for any lower ice class vessel then ULA. The NSIDC-CCAR ice type maps are also sensitive for melting ice. Due to above largest uncertainties should be expected during melting period and in the Marginal Ice Zone. It may be generalized, that all sea ice fields presented on data sources that are developed on basis of weather filter related to 30-40% of sea ice concentration should be considered as "areas to be avoided" by vessels of ice class lower than L1.

The results of the work allow to estimate general correlations in between various kinds of sea ice edges in relation to the distance from sea ice extent line. They are located in the sequence of the following distances: center of "ambiguous" zone presented on OSISAF ice age maps - 21 Nm, center of 30-40% ice floe concentration (IUP product excluded) - 24.1 Nm, center of 70-81-91% ice floe concentration - 30.6 Nm. As the maximal average distance of analysed lines (IUP product excluded) was equal 37.2 Nm, then relative distances in relation to the sea ice extent line were: center of "ambiguous" zone presented on OSISAF ice age maps – 37%, center of 30-40% ice floe concentration (IUP product excluded) - 65%, center of 70-81-91% ice floe concentration - 82%.

Tendencies of distance changes were very well correlated. The lowest distance for line of 30-40% of concentration of sea ice pack was very close to "ambiguous" field limit from Open Water side. Next, the "ambiguous" field limit from 1st year ice was very close to lowest distance for lines 70-81-91% of concentration limit of various sources. Finally, the highest distance for line of 30-40% of concentration of sea ice pack was very close to highest distance for lines 70-81-91% of concentration limit of various sources. In case of shortage of data sources these pairs could be used for estimation of sea ice pack location as equivalency - one line instead of other one. The limit of high concentration ice pack is generally in same position. Discrepancy of location in between 30-40% and 70-81-91% concentration looks be negligible. The width of ice field in between 30-40% and 70-81-91% concentration is higher than 3 Nm only in places of higher volatility of analysed lines, especially where the general course of ice limit direction is considerably changed on longer distances.

Detailed average distances of various analysed lines from external line of ice data in relation to maximal ice data values were found as follow: 8.4 Nm (23%) for NSIDC-CCAR ice age, 12.3 Nm (33%) for

minimal distance of 30-40% ice concentration, 15.4 Nm (41%) for OSISAF ice type "ambiguous" zone from Open Water side, 25 Nm (67%) for minimal distance of 70-81-91% ice concentration 26.6 Nm (72%) for OSISAF ice type "ambiguous" zone from 1st year ice age, 35.9 Nm (97%) for maximal distance of 30-40% ice concentration and 36.3 Nm (98%) for maximal distance of 70-81-91% ice concentration. In the parentheses placed relative distances in between first ice data and highest data including IUP 40% concentration isolines.

Depending on the sources of information used the estimated speed of L3 ice class vessel from 3.3 knots till 5.2 knots at average speed 5.0 knots was received. Estimated speed of L1 ice class vessel ranged from 6.5 knots till 12.1 knots at average speed 9.7 knots. Relative standard deviation of averaged speed for each of L3 and L1 ice class vessel was equal 18%. The highest relative deviations were found up to 50% below the average speed value. The highest relative deviations upward were equal 22%.

The results of the work are not intended to be used for decision making on spot, "on-scene", during direct guiding vessel in ice. It should be useful for initial voyage planning. Results of analysis allow decision-makers to identify the best data sources for considered voyage and vessel of defined ice class; to understand advantages and limitations of freely available in the internet data sources; to estimate vessel's maximal safe speed in encountered ice conditions and to estimate spatial distribution and correlations in between various levels of sea ice concentration and thickness.

ACRONYMS

AARI - Arctic and Antarctic Research Institute in St.Petersburg
ALOS - Advanced Land Observing Satellite
AMSR-E - Advanced Microwave Scanning Radiometer - Earth Observing System
AMSR2 - Advanced Microwave Scanning Radiometer 2
AMSU - Advanced Microwave Sounding Unit
ASA - Advanced Synthetic Aperture Radar
ASI - ARTIST Sea Ice
AVHRR- VIS Advanced Very High Resolution Radiometer
AVHRR-VIS - Advanced Very High Resolution Radiometer - Visible Band
CCAR – Colorado Center of aerodynamics Research
CDAS - Climate Data Assimilation System
CDOP - Continuous Development and Operations Phase by Meteo-France
CERSAT - French ERS Processing and Archiving Facility
CIS - Canadian Ice Service
CT - Concentration Total
DMI - Danish Meteorological Institut
DMSP - Defense Meteorological Satellite Program
DMSP OLS - Defense Meteorological Satellite Progam – Operational Linescan System
ENVISAT - ENVIronmental SATellite
ESIMO - ЕСИМО, Единая Система Информации об обстановке в Мировом Океане
EUMETSAT - EUropean Organisation for the Exploitation of METeorological SATellites
GDSIDB - Global Digital Sea Ice Data Bank
GMM - Geometrical Mathematical Model
GOES - Geostationary Operational Environmental Satellite
IAPB - International Arctic Buoy Program
IFREMER - Institut Français de Recherche pour l'exploitation de la Mer
IMS - Interactive Multisensor Snow and Ice Mapping System
IUP - Institut für Umweltphysik, Universität Bremen
MASIE - Multisensor Analyzed Sea Ice Extent
Met.no - Norwegian Meteorological Institute
MIZ - Mariginal Ice Zone
MMAB - Marine Modeling and Analysis Branch
MODIS - Moderate Resolution Imaging Spectroradiometer
MTSAT - Multi-functional Transport Satellite
NAVO - Naval Oceanographic Office
NCAR - National Center for Atmospheric Research
NCEP - National Centers for Environmental Prediction
NESDIS - National Environmental Satellite, Data, and Information Service
NGDC - National Geophysical Data Center
NIC - National Ice Center, US National Ice Service, US Naval Ice Service
NIS - Norwegian Ice Services
NOAA - National Oceanic and Atmospheric Administration
NOMADS - National Operational Model Archive & Distribution System
NSIDC - National Snow and Ice Data Center
NWP - Numerical Weather Prediction
NWS - National Weather Service
OSISAF - Ocean And Sea Ice Satellite Application Facility, High Latitude Centre
PALSAR - Phased Array type L-band Synthetic Aperture Radar
QUIKSSCAT - "quick recovery" mission from the NASA Scatterometer
RADARSAT - RADAR SATellite system equipped with a powerful synthetic aperture radar
RGB - additive Red, Green, Blue color model
SAF - Satellite Application Facilities
SAR - Synthetic Aperture Radar
SEVIRI - Spinning Enhanced Visible and Infrared Imager
SMHI - Swedish Meteorological and Hydrological Institute
SMMR - Scanning Multichannel Microwave Radiometer
SSM/I - Special Sensor Microwave Imager
SMMIS - Special Sensor Microwave Imager Sounder
UKHO - United Kingdom Hydrographic Office
URL - Uniform Resource Locator

REFERENCES

Arikaynen A. I., 1990. Sudokhodstvo vo l'dakh Arktiki. Moskva "Transport": 247 p.

ArikaynenA.I., Tsubakov K. N., 1987. Azbuka ledovogo plavanija. Transport, Moskva: 224 p.

Erzaty R., Girard-Ardhuin F., Croize-Fillon D., 2007. Sea ice drift in the central arctic using the 89 GHz brightness temperatures of the advanced microvawe scanning radiometer, Users manual. Laboratoire d'Océanographie Spatiale Département d'Océanographie Physique et Spatiale, IFREMER: 20 p.

Timco G. W., Gorman B., Falkingham J., O'Connell B., 2005. Scoping Study: Ice Infor-mation Requirements for Marine Transportation of Natural Gas from the High Arctic. Technical Report CHC-TR-029, Canadian Hydraulics Centre, Ottawa: 124 p.

Russian Maritime Register of Shipping, 2015. Rules for the classification and construction of sea-going ships, Volume 1, Edition 2015, Saint-Petersburg, 492 p.

Rodrigues J., 2009, The increase in the length of the ice-free season in the Arctic. Cold Regions Science and Technology 59 (2009): 78-101.

Maslanik J., Stroeve J., Fowler Ch., Emery W., 2011. Distribution and trends in Arctic sea ice age through spring 2011, Geographical Research Letters, Vol. 38, L13502, doi:10.1029/2011GL047735, 2011, 6 p.

Eastwood E.(editor), 2014. Ocean & Sea Ice SAF Sea Ice Product User's Manual, OSI-401-a, OSI-402-a, OSI-403-a, Version 3.11, 39 p.

Comiso, J.,1999. Bootstrap Sea Ice Concentrations from Nimbus-7 SMMR and DMSP SSM/I. National Snow and Ice Data Center, Boulder, CO. Digital Media (updated 2005).

Canadian Hydraulics Centre, 2003. Arctic Ice Regimę Shipping system, TP14044E (https://www.tc.gc.ca/media/documents/marinesafety/tp14044e_airss_guide.pdf), Transport Canada, 65 p.

Maslanik J. A., Fowler C.,Stroeve J.,Drobot S., Zwally J., Yi D., Emery W., 2007. A younger, thinner Arctic ice cover: Increased potential for rapid, extensive sea-ice loss. Geographical Research Letters, Vol. 34, L24501, doi:10.1029/2007GL032043, 2007.

Mulherin N.D., 1996. The Northern Sea Route. Its development and evolving state of operationsin the 1990s. CRELL Report 96-3, US Army Corps of Engineers: 84 s.